

~~CONFIDENTIAL~~

Copy 8
RM L53L14

NACA RM L53L14



RESEARCH MEMORANDUM

STABILITY CHARACTERISTICS AT LOW SPEED OF A VARIABLE-SWEEP
AIRPLANE MODEL HAVING A PARTIALLY CAMBERED WING
WITH SEVERAL CHORD-EXTENSION CONFIGURATIONS

By Robert E. Becht

Langley Aeronautical Laboratory
Langley Field, Va.

CLASSIFICATION CANCELLED

Author: NACA 102-661 Date 12/17/53

RAF No. 94

By NACA 1/18/54 See

CLASSIFIED DOCUMENT

This material contains information affecting the National Defense of the United States within the meaning of the espionage laws, Title 18, U.S.C., Secs. 793 and 794, the transmission or revelation of which in any manner to an unauthorized person is prohibited by law.

NATIONAL ADVISORY COMMITTEE FOR AERONAUTICS

WASHINGTON
February 12, 1954

LANGLEY FIELD, VIRGINIA

~~CONFIDENTIAL~~



NATIONAL ADVISORY COMMITTEE FOR AERONAUTICS

RESEARCH MEMORANDUM

STABILITY CHARACTERISTICS AT LOW SPEED OF A VARIABLE-SWEEP
AIRPLANE MODEL HAVING A PARTIALLY CAMBERED WING
WITH SEVERAL CHORD-EXTENSION CONFIGURATIONS

By Robert E. Becht

SUMMARY

An investigation was made to determine the effect of several chord-extension configurations at low speed on a variable-sweep airplane model with a partially cambered wing. The tests were made at a Reynolds number of 2×10^6 based on the mean aerodynamic chord of the wing at 50° sweep for average test conditions.

The results of the investigation indicated that the chord-extension having the inboard end location at 0.75 semispan produced the most nearly linear pitching-moment curves at 50° sweep. At 60° sweep, this chord-extension was not the optimum, but the differences were small. The effectiveness of the chord-extension was slightly decreased at all sweep angles when the inboard end was made normal to the wing leading edge. At 20° sweep, all chord-extensions examined caused some reduction in longitudinal stability at high lift coefficients with flaps retracted; but with flaps deflected, essentially no variation in stability with lift coefficient was produced by the chord-extensions. The effective dihedral was increased at intermediate lift coefficients of the wing at all sweep angles by the chord-extensions, but a more negative value was obtained just before stall of the wing at 60° sweep.

INTRODUCTION

A previous investigation of the aerodynamic characteristics of a model, representative of a variable-sweep airplane, showed that performance gains could be realized with a wing having partial-span leading-edge camber in preference to a wing having symmetrical sections. (See ref. 1.) However, the model with either of the two wings exhibited the adverse stability characteristics associated with thin wings of moderate or high sweep angles, that is, a reduction in longitudinal stability at intermediate or high lift coefficients.



The present paper contains the results of an investigation at low speed of several chord-extension configurations used in an attempt to improve the stability characteristics of the model having the partial-span cambered leading-edge wing. Data are presented at wing sweep angles of 20° , 50° , and 60° . In addition, the stability characteristics of the model having either a wing of symmetrical sections and slats or a partial-span cambered leading-edge wing with chord-extensions are discussed using the characteristics of the model with the symmetrical wing as a basis for comparison. (See ref. 2.)

SYMBOLS

The system of axes employed, together with the positive direction of the forces, moments, and angles, is given in figure 1. The aerodynamic force and moment coefficients are based on the actual wing area and span which vary with sweep angle, but a constant chord equal to the wing mean aerodynamic chord at 50° sweep is used for the pitching-moment coefficients. The pitching moments were measured about a fixed fuselage station. The wing translated so that for any sweep angle the quarter-chord point of the mean aerodynamic chord fell at this same fuselage station. (See fig. 2.) The symbols used are defined as follows:

C_L	lift coefficient, $Lift/qS$
C_X	longitudinal-force coefficient, X/qS
C_Y	lateral-force coefficient, Y/qS
C_l	rolling-moment coefficient, L/qSb
C_m	pitching-moment coefficient, $M/qS\bar{c}_{50}$
C_n	yawing-moment coefficient, N/qSb
X	longitudinal force along X-axis (Drag = $-X$), lb
Y	lateral force along Y-axis, lb
Z	force along Z-axis (Lift = $-Z$), lb
L	rolling moment about X-axis, ft-lb
M	pitching moment about Y-axis, ft-lb

- N yawing moment about Z-axis, ft-lb
- q free-stream dynamic pressure, $\rho V^2/2$, lb/sq ft
- S wing area, sq ft
- \bar{c} wing mean aerodynamic chord, $\frac{\int_0^{b/2} c'^2 dy}{\int_0^{b/2} c' dy}$, ft; based on plan forms shown in figure 2
- \bar{c}_{50} wing mean aerodynamic chord at 50° sweep, ft
- c' local streamwise chord, ft
- c local wing chord perpendicular to quarter-chord line of unswept wing, ft
- b wing span, ft
- V free-stream velocity, fps
- A aspect ratio, b^2/S
- ρ mass density of air, slugs/cu ft
- α angle of attack of thrust line, deg
- β angle of sideslip, deg
- i_t angle of incidence of stabilizer with respect to thrust line, deg
- δ_f flap deflection measured in plane perpendicular to hinge line, deg
- Λ angle of sweep of quarter-chord line of unswept wing, deg
- y spanwise distance measured perpendicular to plane of symmetry, ft
- d streamwise distance back of local wing leading edge, ft

Subscript:

β partial derivative of a coefficient with respect to sideslip angle; for example, $C_{l\beta} = \partial C_l / \partial \beta$

MODEL

The physical characteristics of the model are presented in figure 2 and a photograph of the model on the support strut is given in figure 3. Figure 4 shows the details of the split flaps and figure 5 shows the details of the chord-extensions. A 12-percent extension of the local chord of the wing at 50° sweep was used and the following table lists the chord-extension configurations investigated:

Chord-extension number	Spanwise location at $\Lambda = 50^\circ$	Inboard end	Inboard-end shape
1	0.65b/2 to tip	Streamwise at $\Lambda = 50^\circ$	Flat
2	.70b/2 to tip	Streamwise at $\Lambda = 50^\circ$	Flat
3	.75b/2 to tip	Streamwise at $\Lambda = 50^\circ$	Flat
4	.75b/2 to tip	Perpendicular to leading edge	Surface of revolution
5	.75b/2 to tip	Streamwise at $\Lambda = 50^\circ$	Surface of revolution
6	.75b/2 to tip	Streamwise at $\Lambda = 60^\circ$	Flat
7	.80b/2 to tip	Streamwise at $\Lambda = 60^\circ$	Flat

The model was constructed of wood bonded to steel reinforcing members and was the same model as that used in the tests of reference 1.

The wing sections inboard of the 40-percent semispan station and behind the 45-percent-chord line outboard of this semispan station were symmetrical. The remaining portion of the wing was cambered. A plot of the camber line at two semispan stations of the 50° swept wing is presented in figure 6. The thickness distribution measured in planes normal to the 0.25-chord line of the unswept wing was NACA 64(10)-010.3 at the root and tapered to NACA 64-008 at the tip.

The wings were pivoted about axes parallel to the plane of symmetry and normal to the chord plane of the symmetrical sections so that the sweep angle could be varied continuously from 20° to 60°. The incidence of this chord plane measured in a streamwise direction was zero.

A jet-engine duct was simulated on the model by use of an open tube having an inside diameter equal to that of the jet exit and extending from the nose to the jet exit.

TESTS

The tests were made in the Langley 300 MPH 7- by 10-foot tunnel at a dynamic pressure of 34.15 lb/sq ft, which corresponds to a Mach number of 0.152 and a Reynolds number of 2×10^6 based on the mean aerodynamic chord at 50° sweep for average test conditions.

During the tests, no control was imposed on the quantity of air flow through the jet duct. Measurements made in previous tests indicate that the inlet velocity ratio varied between 0.78 and 0.86 - the higher values being observed at low angles of attack.

The parameters $C_{n\beta}$, $C_{Y\beta}$, and $C_{l\beta}$ were determined from tests through the angle-of-attack range at sideslip angles of $\pm 5^\circ$.

CORRECTIONS

The angle-of-attack, drag, and pitching-moment results have been corrected for jet boundary effects that were computed on the basis of an unswept wing theory by the method of reference 3. All coefficients have been corrected for blocking due to the model and its wake by the method of reference 4.

Corrections for the tare forces and moments produced by the support strut have not been applied. It is believed, however, that the significant tare corrections would be limited to small increments in pitching moment and drag.

Vertical buoyancy on the support strut, tunnel air-flow misalignment, and the longitudinal pressure gradient have been accounted for in computation of test data.

PRESENTATION OF DATA

The results of the investigation are presented in the figures listed as follows:

	Figure
Stability characteristics of model with wing of symmetrical sections or wing with partial-span leading-edge camber	7
Effect of chord-extensions on longitudinal stability of model with partial-span cambered leading-edge wing:	
50° sweep	8 and 9
60° sweep	10 and 11
20° sweep	12 and 13
Effect of chord-extensions in conjunction with flaps on longitudinal stability of model with partial-span cambered leading-edge wing:	
20° sweep	14
Effect of chord-extensions on lateral stability parameters of model with partial-span cambered leading-edge wing	15
Effect of several wing modifications on longitudinal and lateral stability of test model	16 and 17

DISCUSSION

The cambered wing provides a performance gain at low sweep angles but also causes more adverse longitudinal stability at high sweep angles. (See fig. 7.) The discussion to follow presents the results of an attempt to improve the longitudinal stability at high sweep angles and still retain the beneficial effects of the cambered leading-edge wing through the use of several chord-extension configurations.

Effect of Chord-Extensions at 50° Sweep

The marked reduction in the stability of the model with the cambered leading-edge wing at 50° sweep was reversed by chord-extensions 1, 2, or 3 - with the increase in stability occurring initially at a lift coefficient of about 0.75. (See fig. 8.) Although the differences in the data obtained with the various chord-extensions were small, chord-extension 3 (inboard end flat and streamwise) showed the smallest stability variation with lift coefficient. A study of figures 8 and 9 indicates that an increase in the stability of the wing-fuselage combination and a reduction in the effective downwash at the tail of the complete model contribute to this improved stability variation with lift coefficient. Chord-extension 4 (inboard end perpendicular to wing leading edge) had no effect on the increase in stability at $C_L \approx 0.75$, but unstable pitching moments were again obtained near the stall. Inasmuch as chord-extension 3 appeared to be the optimum configuration investigated for this sweep angle, it will be used as the basis of comparison for the other sweep angles which follow.

Effect of Chord-Extensions at 60° Sweep

The effect of chord-extensions 3 to 7 on the longitudinal stability of the model with the wing at 60° sweep is presented in figure 10. It can be seen that chord-extension 3 (inboard end flat and streamwise at 50° sweep) again considerably improved the longitudinal stability of the model with the clean wing. However, a slight destabilizing break in the pitching-moment curve was noted at lift coefficients just below stall which was more pronounced with chord-extension 4 (inboard end perpendicular to the wing leading edge). This reduction in stability was eliminated by use of chord-extension 5 (inboard end a surface of revolution and streamwise at $\Lambda = 50^\circ$). The data obtained with chord-extensions 6 and 7 show that neither was as effective as 5 in providing a linear pitching-moment variation with lift coefficient below the stall. It was also noted that a greater improvement in the tail-off stability variation with lift coefficient was obtained with chord-extension 3 at 60° sweep than at 50° sweep. (See fig. 11.)

Effect of Chord-Extensions at 20° Sweep

Figure 12 shows that chord-extensions 3, 4, and 5 produced noticeable reductions of about the same magnitude rather than increases in the longitudinal stability of the complete model at intermediate and high lift coefficients of the wing at 20° sweep. In fact, for the center-of-gravity location chosen, the model with chord-extensions was essentially neutrally stable from $C_L \approx 0.7$ to the stall. Inasmuch as

the stability characteristics of the model with the horizontal tail off were only slightly reduced by the addition of a chord-extension (see fig. 13), an increase in effective downwash at the tail probably accounts to some extent for the reduction in longitudinal stability of the complete model.

The reduction in longitudinal stability at intermediate and high lift coefficients of the wing at 20° sweep - as obtained on the complete model with chord-extensions and with flaps up - was not obtained with the configuration having chord-extensions but with flaps down. (See fig. 14.) Except for a slight nose-up trim change, essentially the same effect was obtained on the model with flaps down and with drooped chord-extensions. The drooped chord-extension also produced a noticeable reduction in drag due to lift, part of which probably resulted from the increased camber effect of the drooped leading edge. With the partial-span flaps deflected, drooping the chord-extension produced essentially no increase in $C_{L_{max}}$. It was noted, however, that the undrooped chord-extensions produced an increase in $C_{L_{max}}$ when added to the clean wing and about twice this increase when added to the wing with flaps down.

Effect of Chord-Extensions on Lateral Stability

The effective dihedral was increased at intermediate lift coefficients of the wing at all sweep angles and also at lift coefficients just below stall for 20° and 50° sweep by use of chord-extension 3. (See fig. 15.) A more negative effective dihedral, however, was produced by the chord-extensions at lift coefficients just below stall of the wing at 60° sweep. In all other respects, the lateral stability characteristics were essentially unchanged by use of chord-extensions.

Comparison of Characteristics With Different Wing Modifications

The previous discussion showed that the addition of chord-extension 3 (inboard end flat) to the cambered leading-edge wing resulted in a considerable improvement in the longitudinal stability of the complete model at high sweep angles. Although chord-extension 5 (inboard end faired to a surface of revolution) was slightly superior to chord-extension 3 in linearizing the pitching moments at 60° sweep, the data with chord-extension 3 are more complete and will, therefore, be used in the comparisons which follow.

The nonlinearities in the longitudinal stability variation with lift coefficient of the model with the symmetrical wing at 60° sweep were about equally reduced by either slats or leading-edge camber and chord-extensions. (See fig. 16.) At 20° sweep, the slats on the symmetrical

wing gave a slightly better variation of stability with lift coefficient than the cambered leading-edge wing with chord-extensions. In addition, the increase in $C_{L_{max}}$ produced by the slats was about twice that obtained with the leading-edge camber and chord-extensions.

The effective dihedral of the model with the symmetrical wing at 60° sweep was appreciably increased in the intermediate lift-coefficient range by use of the partial-span leading-edge camber and chord-extensions. (See fig. 17.) In general, these increases were almost doubled by the slats. Near the stall, the partial-span cambered leading-edge wing with chord-extensions produced higher negative values of effective dihedral than were obtained with the symmetrical wing; whereas the slats produced positive values through the entire lift-coefficient range.

At 20° sweep, the slats produced a slight reduction in effective dihedral in the lift-coefficient range below the stall of the model with the symmetrical wing. The cambered leading-edge wing with chord-extensions produced no significant changes in effective dihedral in this same lift-coefficient range, except for some increase near the stall. At the stall of each of the modified configurations, the same trends that were obtained at 60° sweep were also apparent at 20° sweep; that is, the slats produced increases in effective dihedral, whereas the leading-edge camber and chord-extensions produced reductions.

The directional stability at 60° sweep was essentially the same for the model with any of the wings investigated. The configuration having slats, however, increased the lift coefficient at which directional instability occurred, although the slats did not appreciably increase $C_{L_{max}}$. In addition, the negative values of directional stability obtained near the stall of the configuration with slats were about half those obtained with the other wing plan forms.

At 20° sweep, except for extending directional stability to higher lift coefficients as a result of increases in $C_{L_{max}}$, the slats on the symmetrical wing or the cambered leading-edge wing with chord-extensions produced essentially the same variation of stability as the plain symmetrical wing.

Although the results at this low Mach number indicate that the modification consisting of leading-edge camber and chord-extensions was not as effective as slats in alleviating the undesirable longitudinal and lateral stability characteristics associated with thin highly swept wings, these trends may not hold through the Mach number range. In addition, it is realized that it is difficult to determine accurately the pitch-up characteristics of the model from static-stability results such as those presented herein. A more complete analysis of this behavior would require the use of the methods presented in reference 5.

CONCLUDING REMARKS

An investigation was made to determine the effect of several chord-extension configurations on the low-speed stability characteristics of a variable-sweep airplane model having a partially cambered wing. The tests were made at a Reynolds number of 2×10^6 based on the mean aerodynamic chord of the wing at 50° sweep for average test conditions.

The chord-extension having the inboard end flat and streamwise at 0.75 semispan was found to give the least variation of longitudinal stability with lift coefficient at 50° sweep. This chord-extension was not the optimum configuration investigated at 60° sweep, but the difference appeared to be small. The effectiveness of the chord-extension was slightly decreased at all sweep angles when the inboard end was made normal to the wing leading edge. At 20° sweep, all chord-extensions examined caused some reduction in stability at high lift coefficients with flaps retracted; but, with flaps deflected, essentially no variation of stability with lift coefficient was produced by the chord-extensions. The effective dihedral was increased at intermediate lift coefficients of the wing at all sweep angles by the chord-extensions, but a more negative value was obtained just below stall of the wing at 60° sweep.

In general, at the low Mach number of this investigation, the overall stability characteristics of the model with the partially cambered wing and chord-extensions were inferior to those obtained with the symmetrical wing and slats.

Langley Aeronautical Laboratory,
National Advisory Committee for Aeronautics,
Langley Field, Va., November 25, 1953.

REFERENCES

1. Becht, Robert E., and Byrnes, Andrew L., Jr.: Investigation of the Low-Speed Aerodynamic Characteristics of a Variable-Sweep Airplane Model With a Wing Having Partial-Span Cambered-Leading-Edge Modifications. NACA RM L52G08a, 1952.
2. Kemp, William B., Jr., Becht, Robert E., and Few, Albert G., Jr.: Stability and Control Characteristics at Low Speed of a $\frac{1}{4}$ -Scale Bell X-5 Airplane Model. Longitudinal Stability and Control. NACA RM L9K08, 1950.
3. Gillis, Clarence L., Polhamus, Edward C., and Gray, Joseph L., Jr.: Charts for Determining Jet-Boundary Corrections for Complete Models in 7- by 10-Foot Closed Rectangular Wind Tunnels. NACA WR L-123, 1945. (Formerly NACA ARR L5G31.)
4. Herriot, John G.: Blockage Corrections for Three-Dimensional-Flow Closed-Throat Wind Tunnels, With Consideration of the Effect of Compressibility. NACA Rep. 995, 1950. (Supersedes NACA RM A7B28.)
5. Campbell, George S., and Weil, Joseph: The Interpretation of Non-linear Pitching Moments in Relation to the Pitch-Up Problem. NACA RM L53I02, 1953.

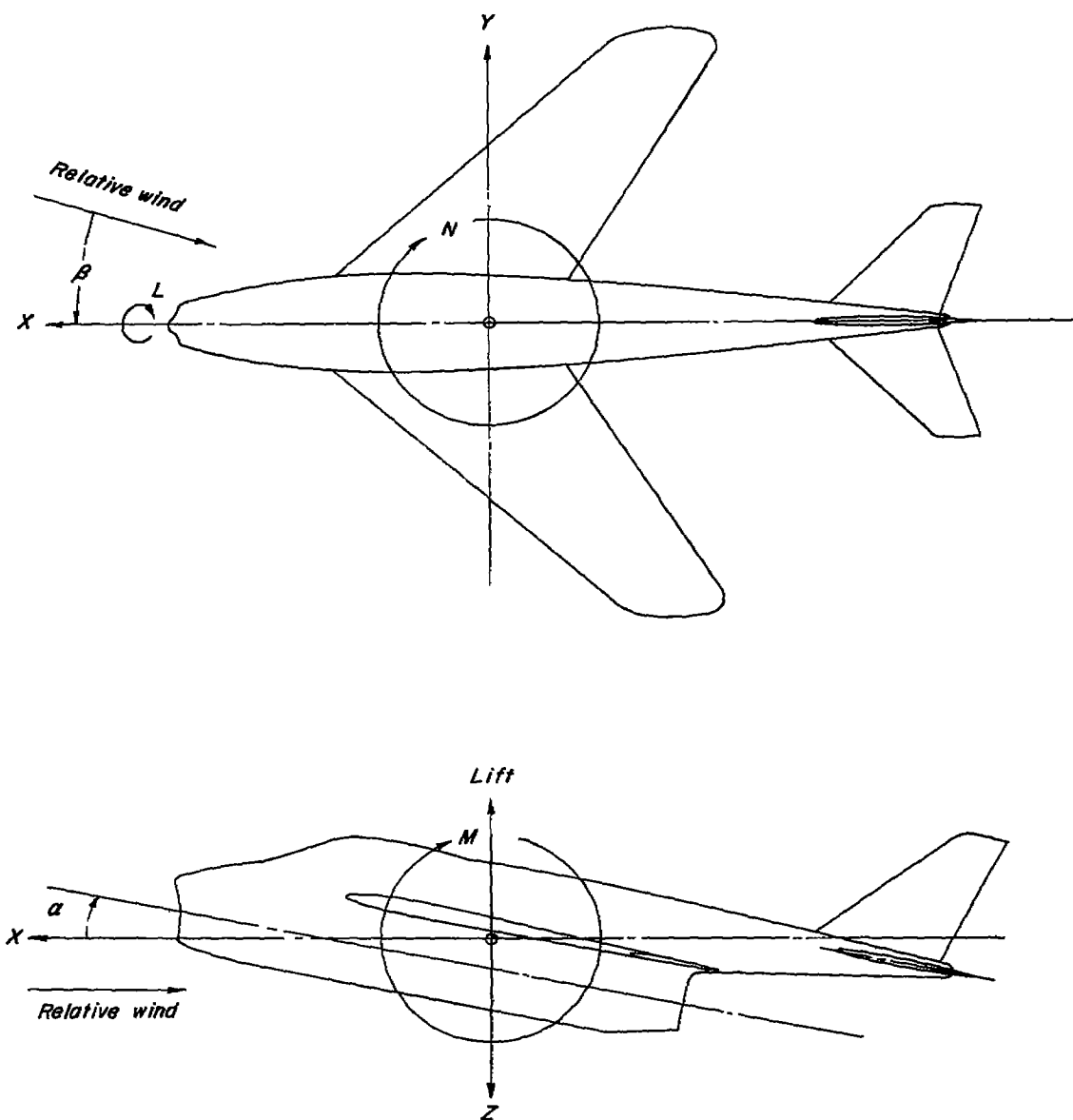
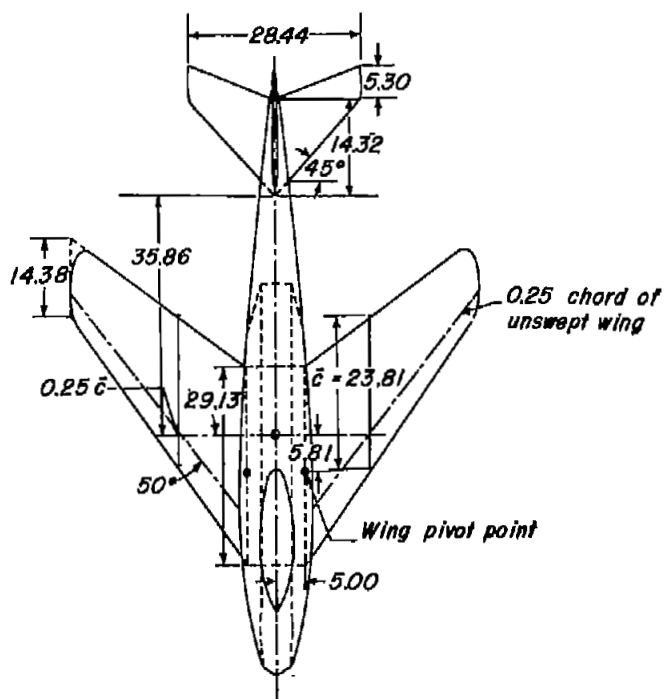


Figure 1.- System of axes. Positive direction of forces, moments, and angles are indicated by arrows.



Physical characteristics

Wing:

<i>Sweep, deg</i>	20	50	60
<i>Area, sqft</i>	10.33	10.80	11.33
<i>Aspect ratio</i>	5.76	2.98	1.92
<i>Span, ft</i>	7.72	5.67	4.66
<i>Mean aerodynamic chord, ft.</i>	1.396	1.985	2.535
<i>Incidence at M.A.C., deg</i>	0.60	0	0.10
<i>Dihedral, deg</i>	-2	-2	-2

Horizontal tail:

<i>Area, sqft</i>	1.94
<i>Aspect ratio</i>	2.89

Vertical tail:

<i>Area, sqft</i>	1.33
<i>Aspect ratio</i>	1.46

0 10 20
Scale, inches

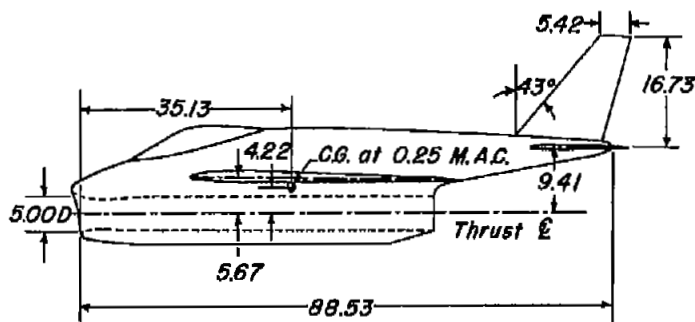
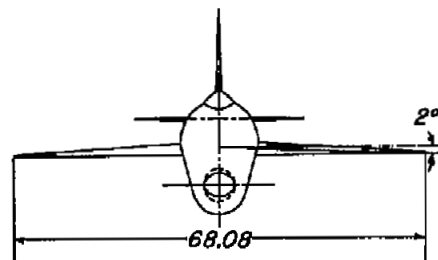


Figure 2.- General arrangement of test model.

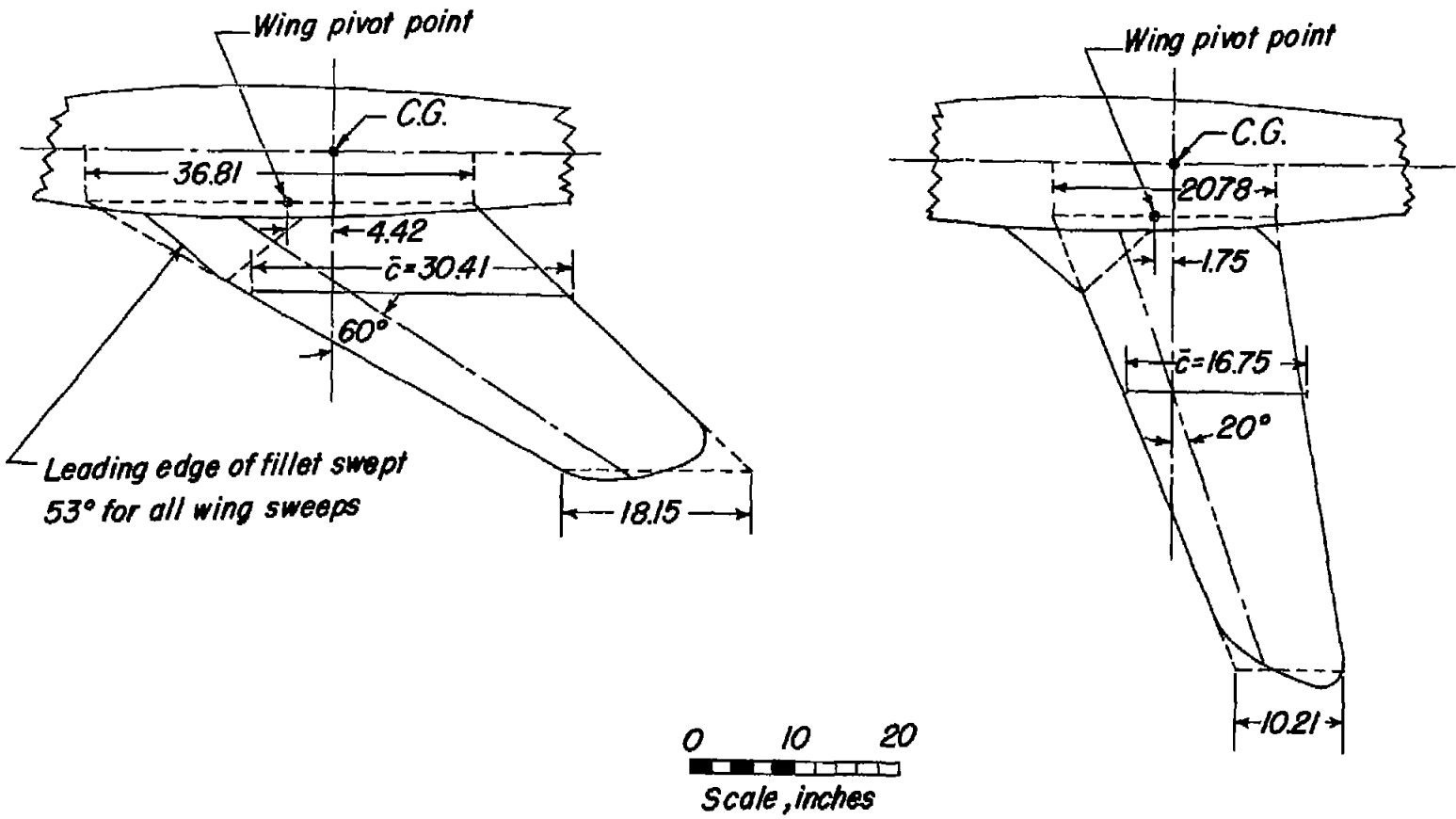
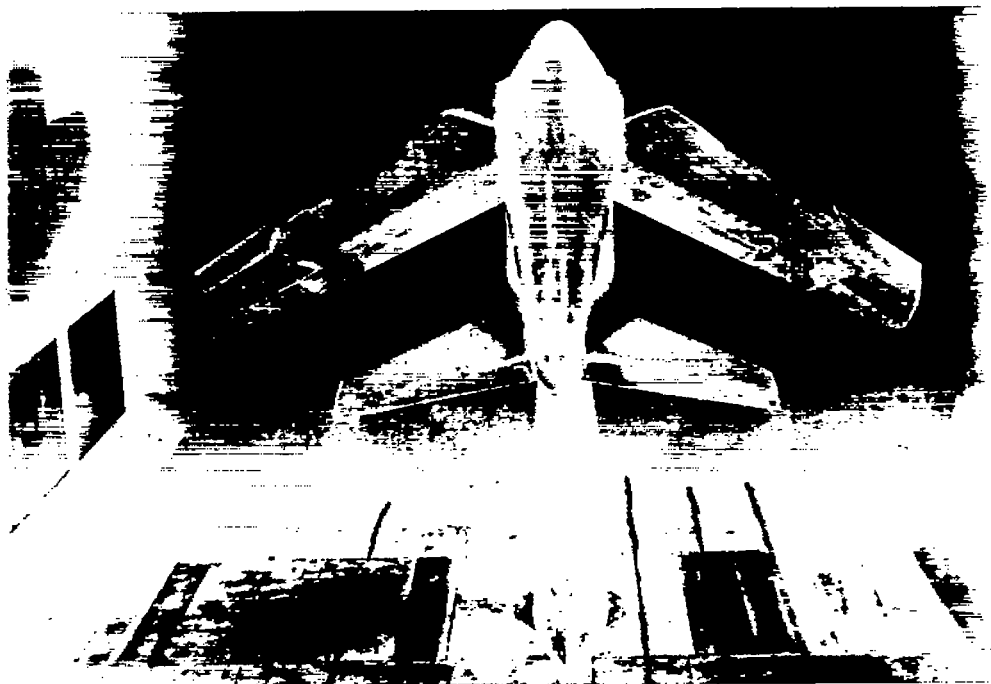


Figure 2.- Concluded.



L-81051



L-81050

Figure 3.- Views of test model mounted on support strut in tunnel.

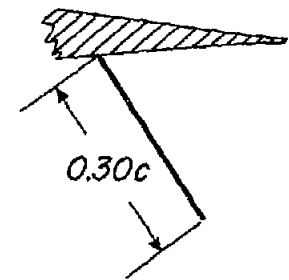
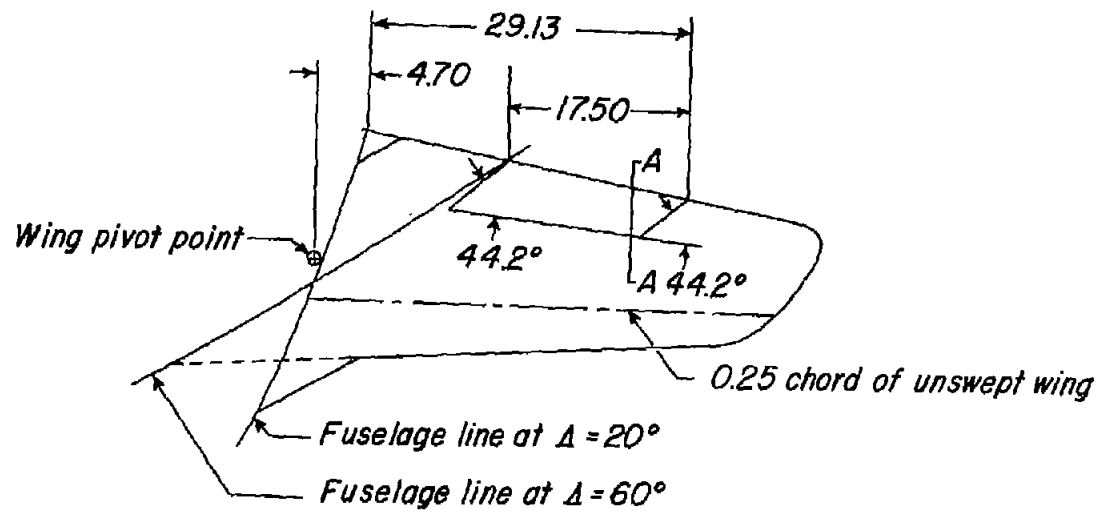
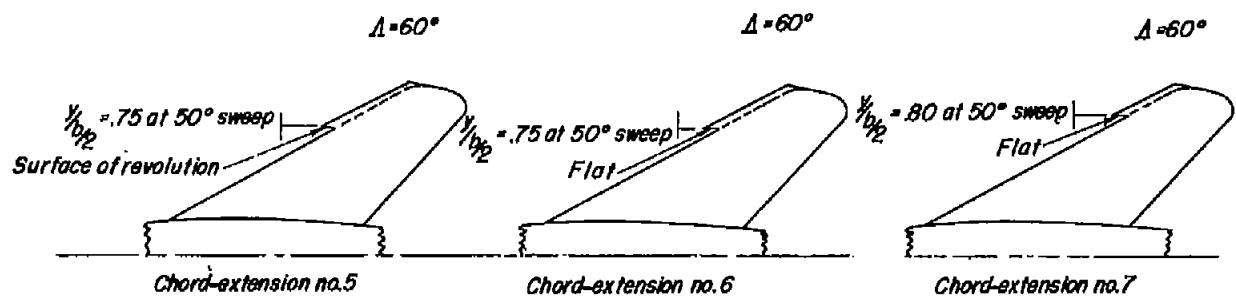
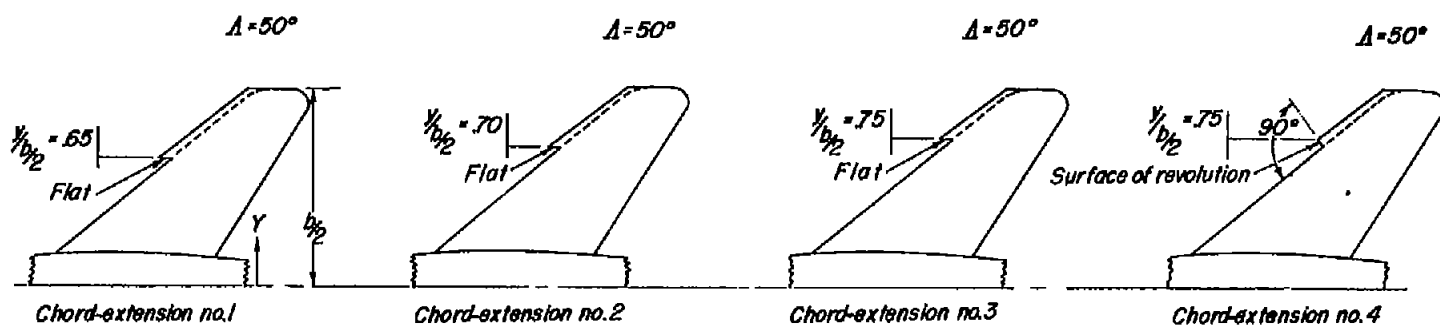


Figure 4.- Details of split flap.



Typical cross section at $y/b_p = .90$; $\Delta=50^\circ$

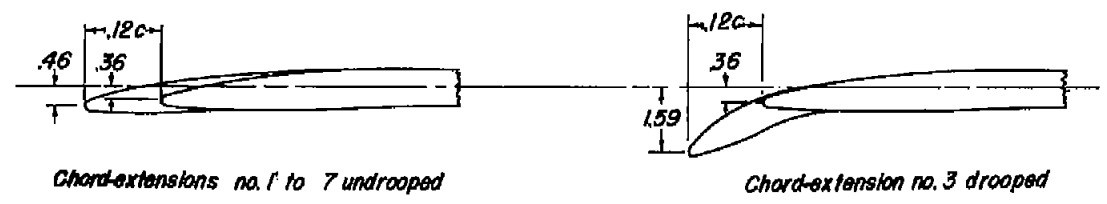


Figure 5.- Details of chord-extensions.

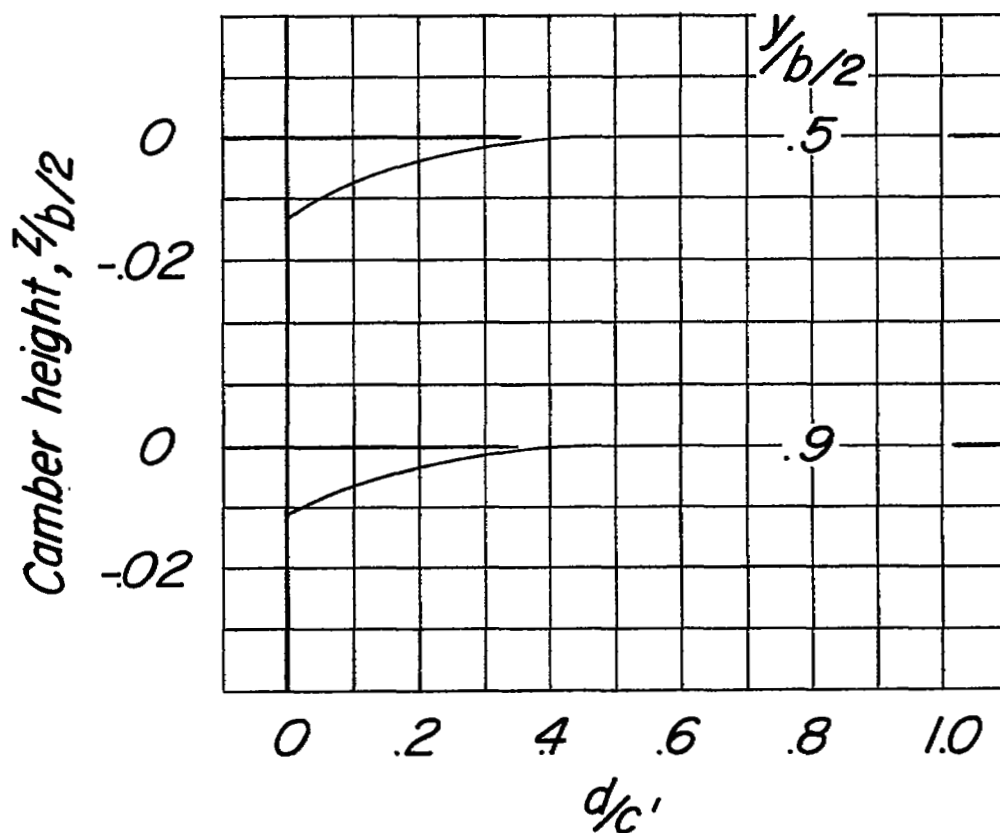
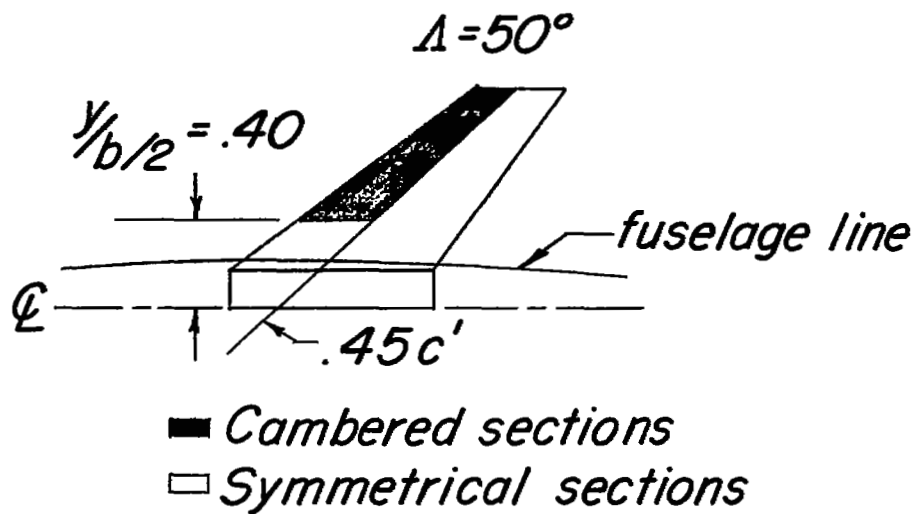


Figure 6.- Variation of wing mean camber height with streamwise chord at 50° sweep.

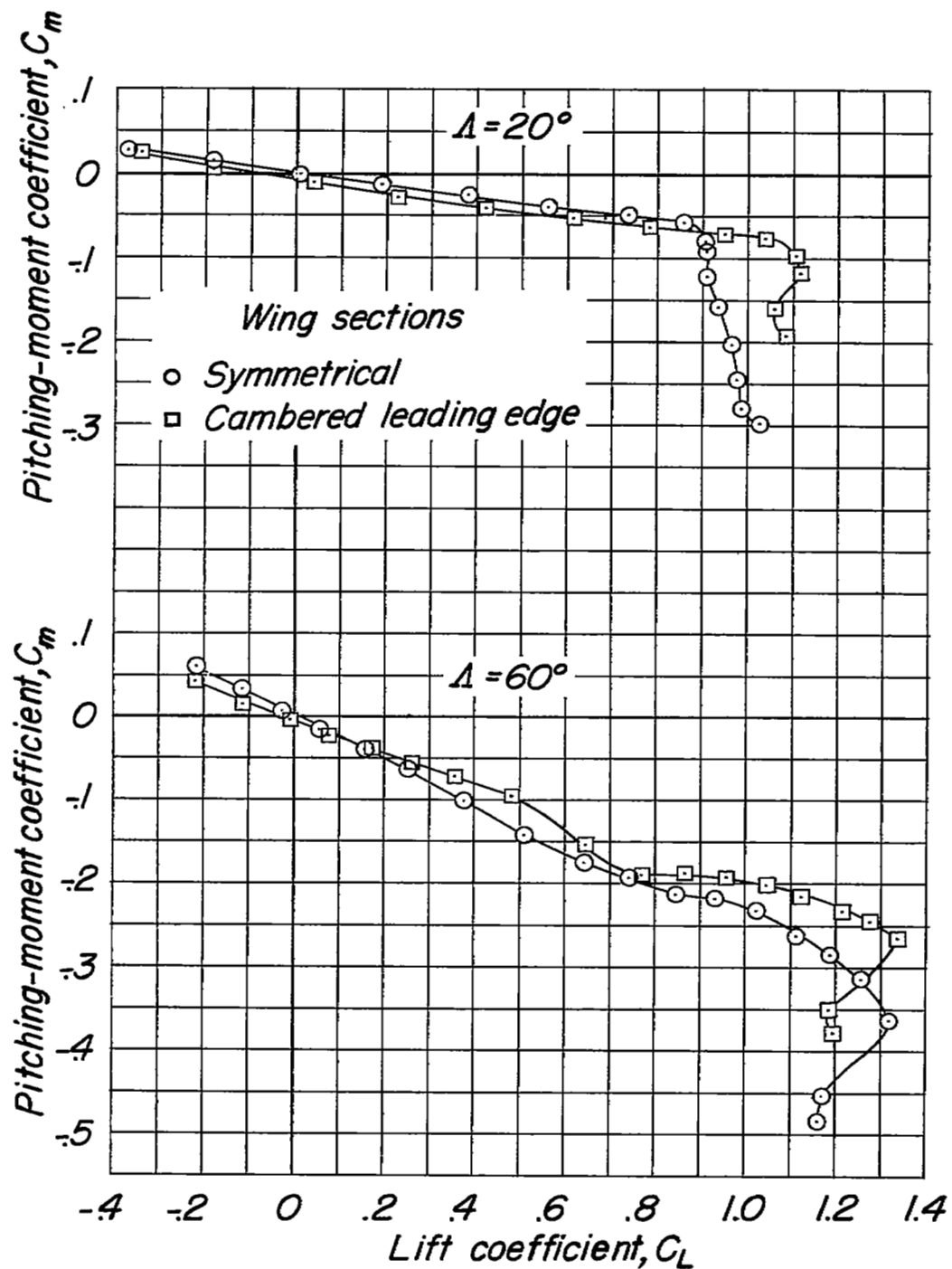
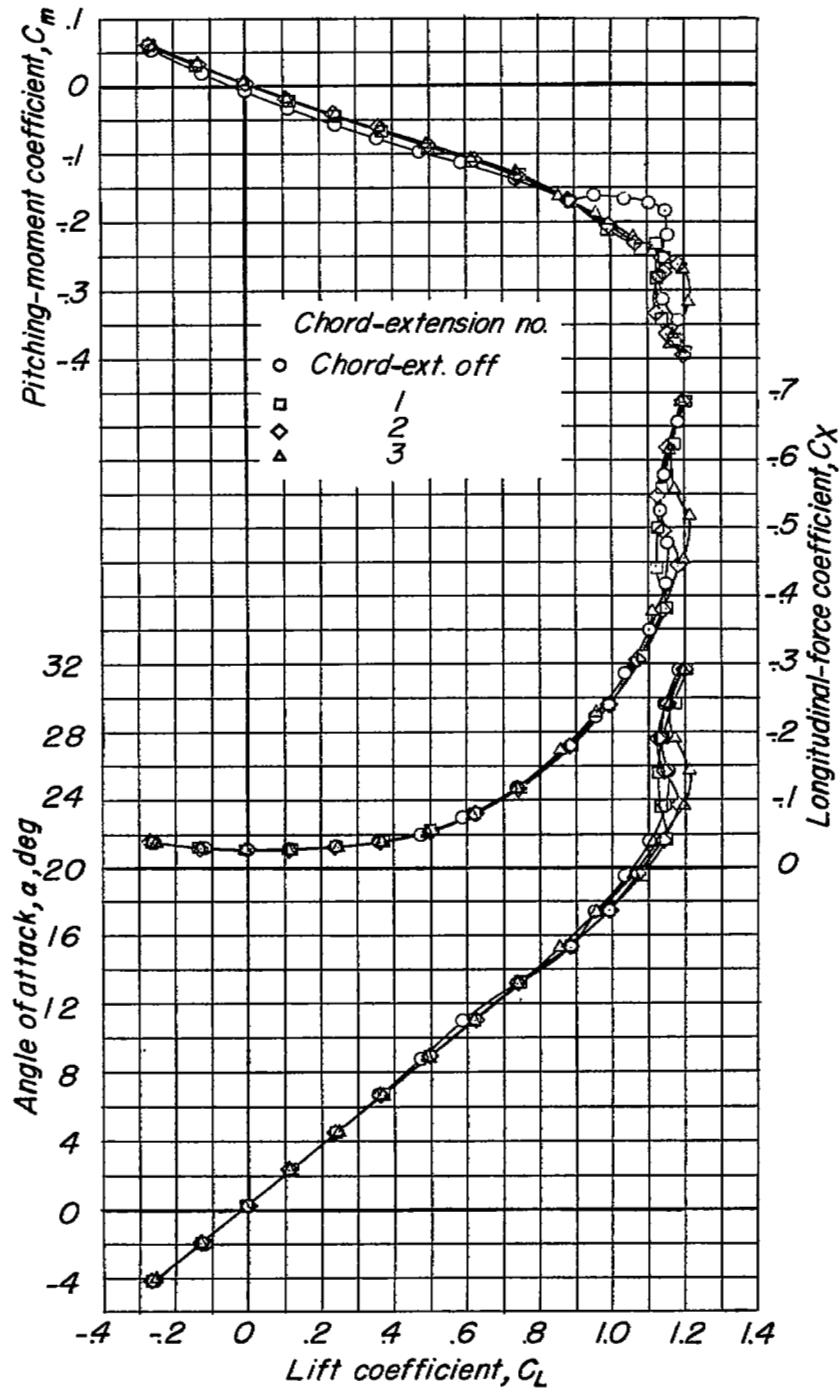
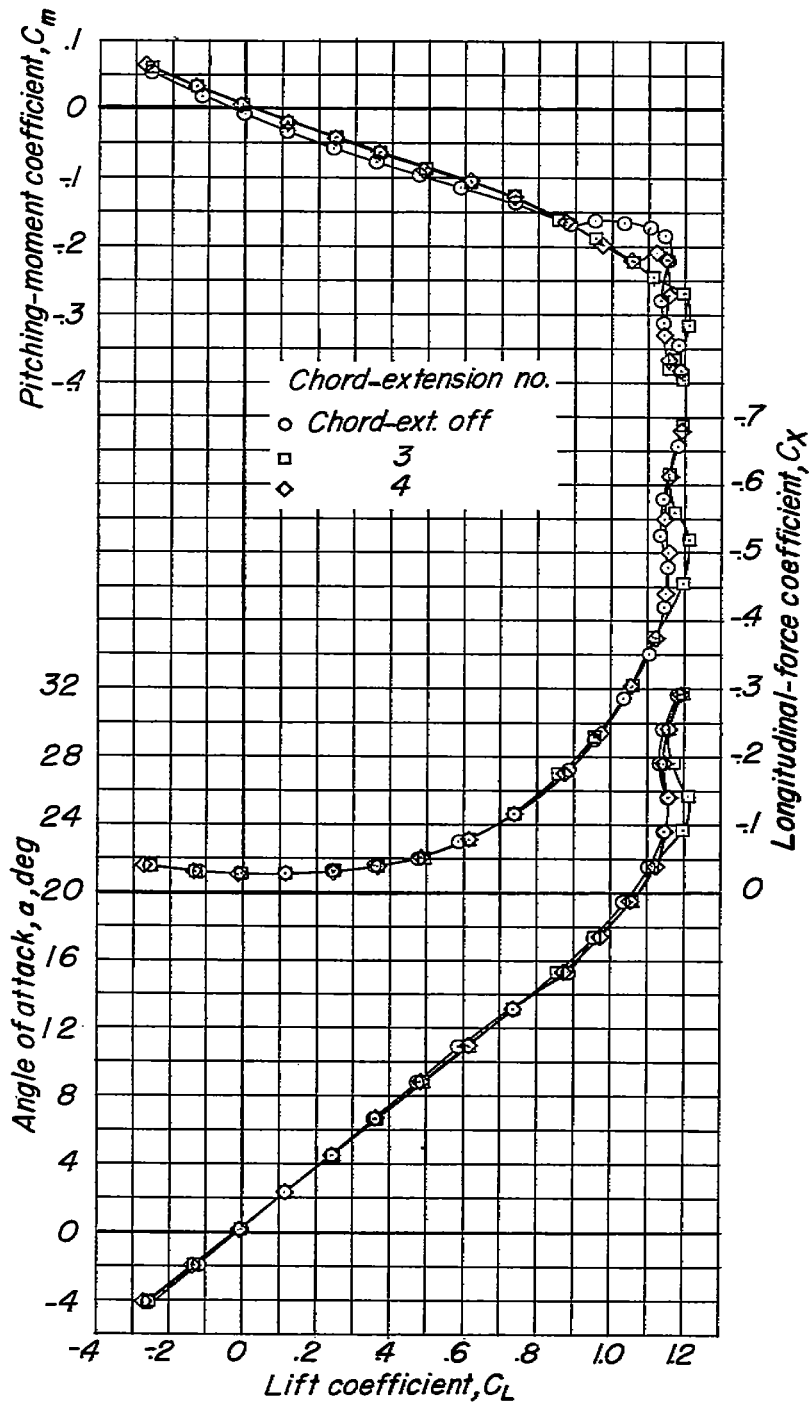


Figure 7.- Longitudinal stability characteristics of model with wing of symmetrical sections or a wing with cambered leading-edge sections, $i_t = -3/4^\circ$; $\delta_f = 0^\circ$.



(a) Chord-extensions off and chord-extensions 1, 2, and 3.

Figure 8.- Effect of several chord-extension configurations on longitudinal aerodynamic characteristics of test model. $\Lambda = 50^\circ$; $i_t = -3/4^\circ$; $\delta_f = 0^\circ$.



(b) Chord-extensions off and chord-extensions 3 and 4.

Figure 8.- Concluded.

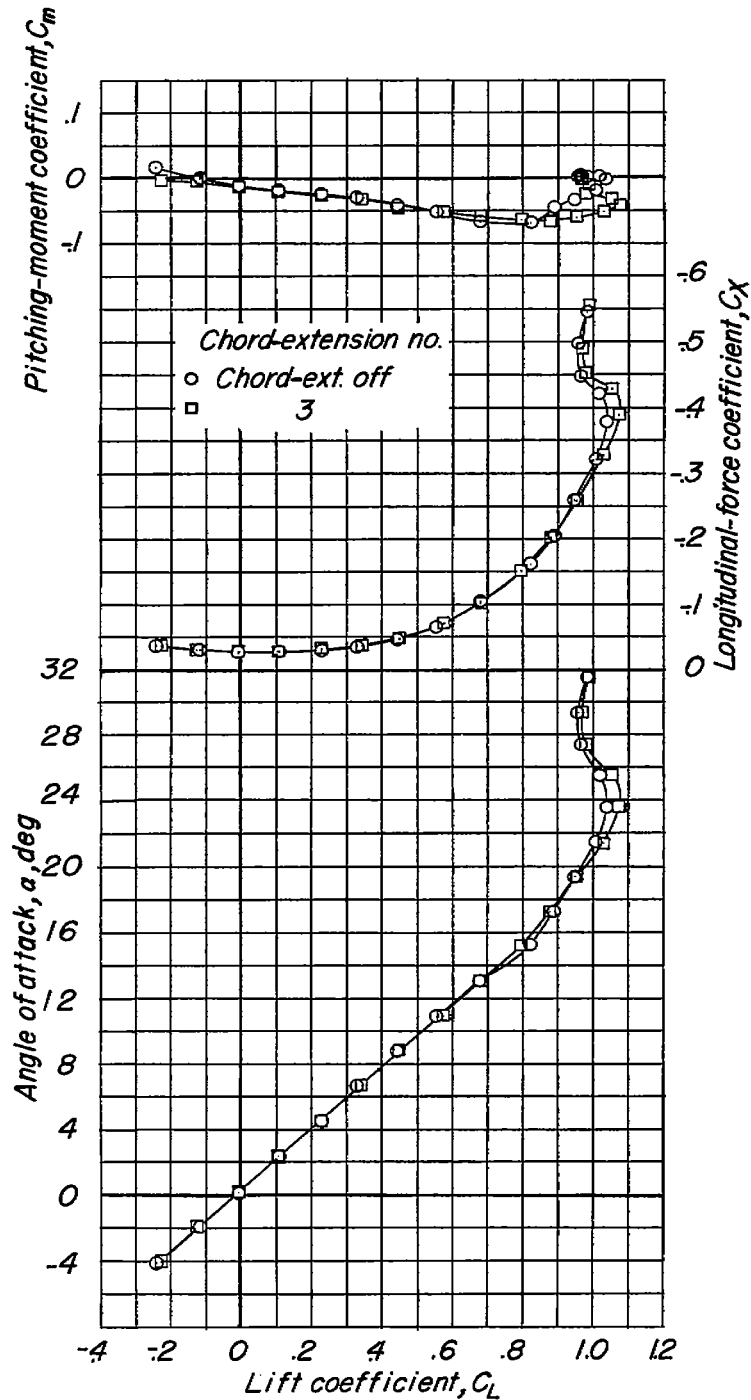
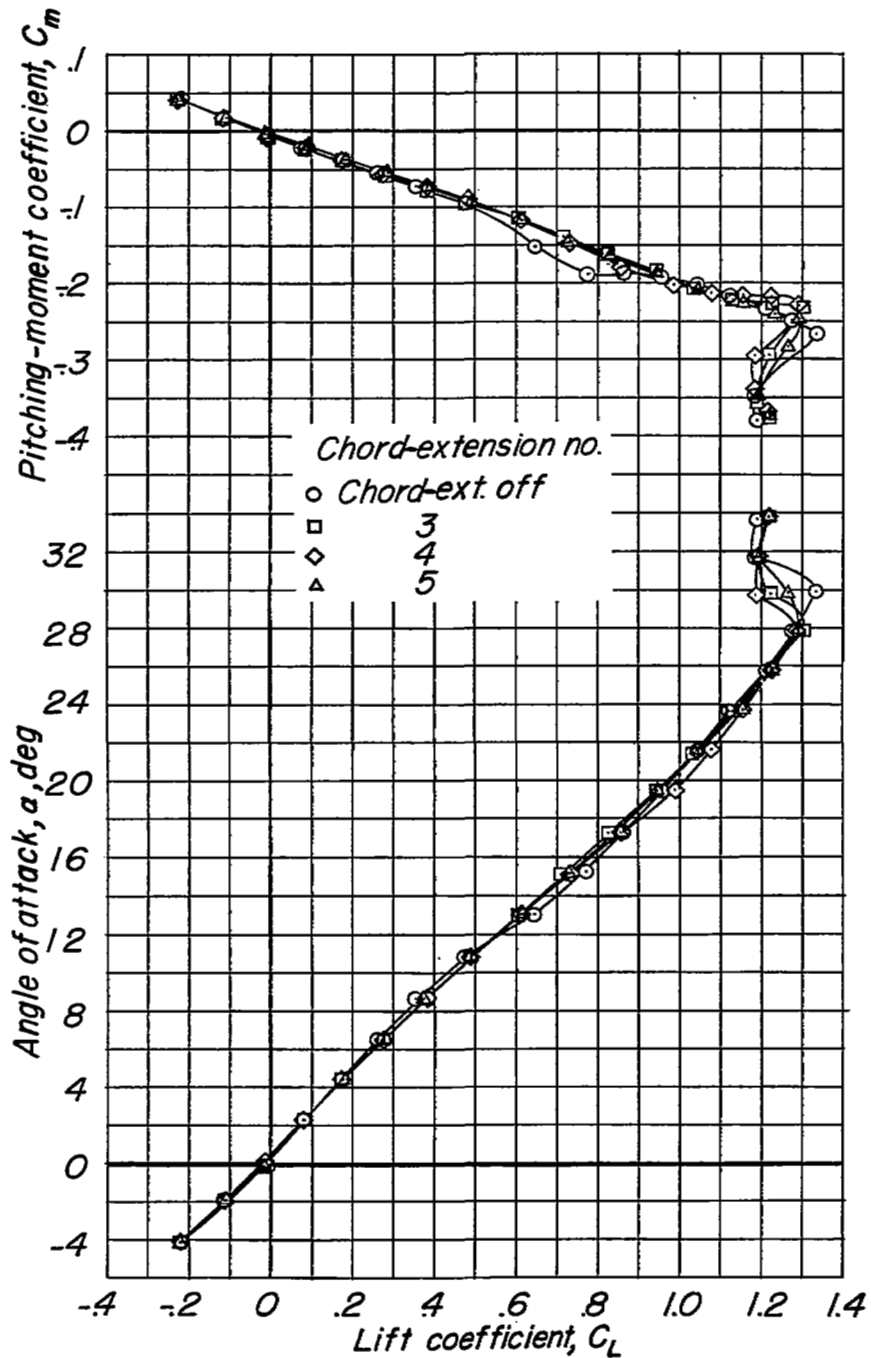
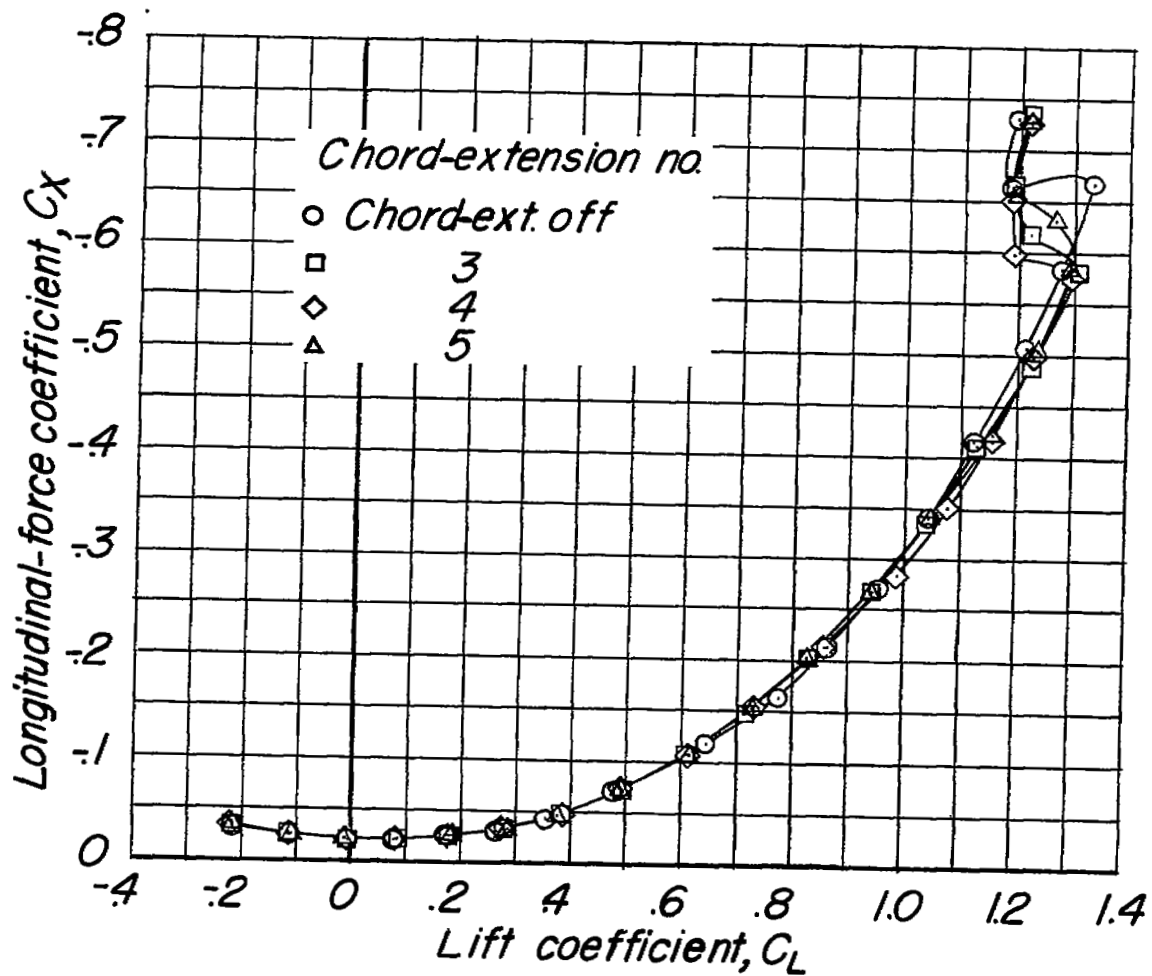


Figure 9.- Effect of chord-extension 3 (inboard end flat and streamwise) on longitudinal aerodynamic characteristics of test model. $\Lambda = 50^\circ$; horizontal tail off; $\delta_f = 0^\circ$.



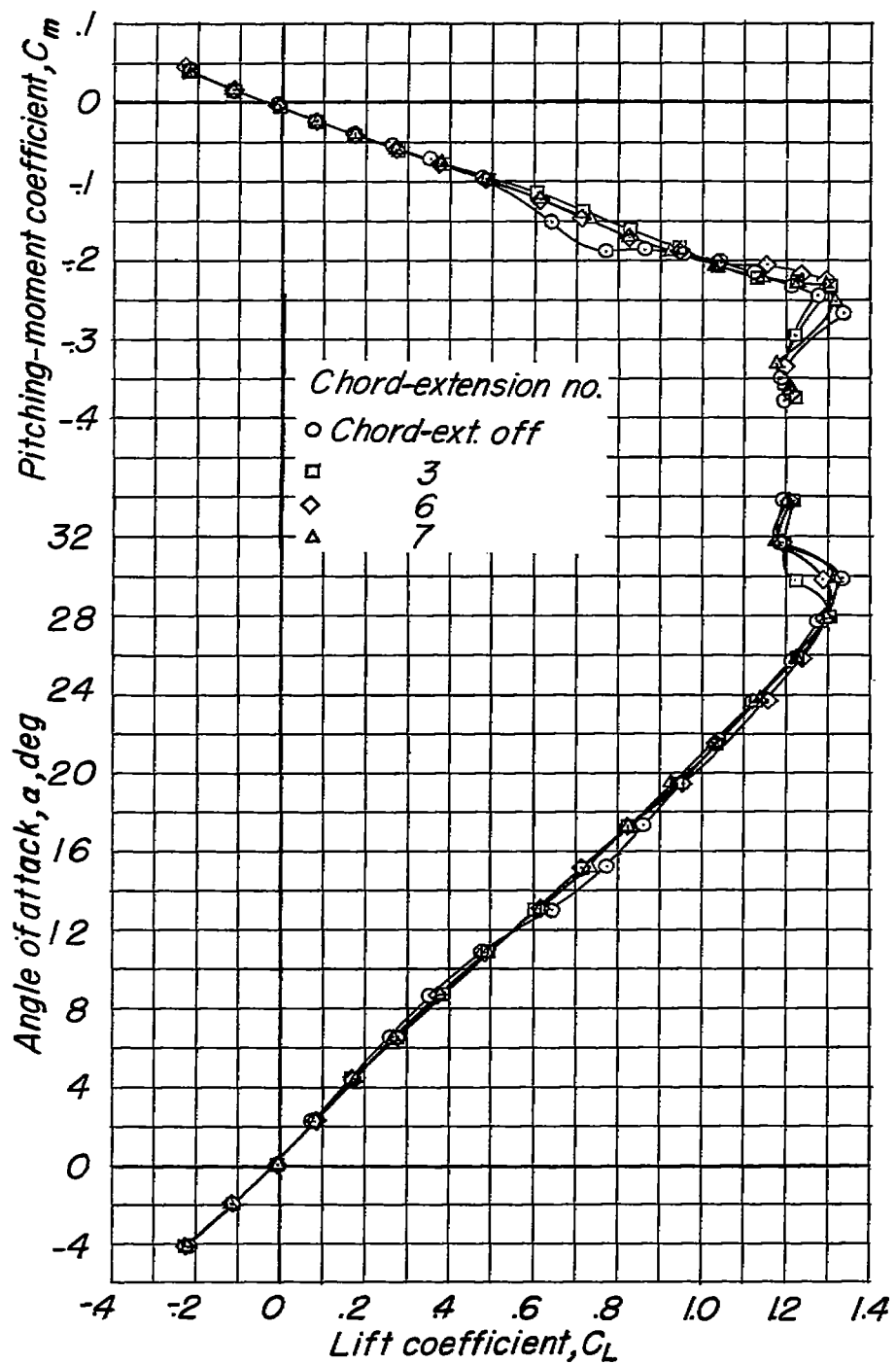
(a) Chord-extensions off and chord-extensions 3, 4, and 5.

Figure 10.- Effect of several chord-extension configurations on longitudinal aerodynamic characteristics of test model. $\Lambda = 60^\circ$; $i_t = -3/4^\circ$; $\delta_f = 0^\circ$.



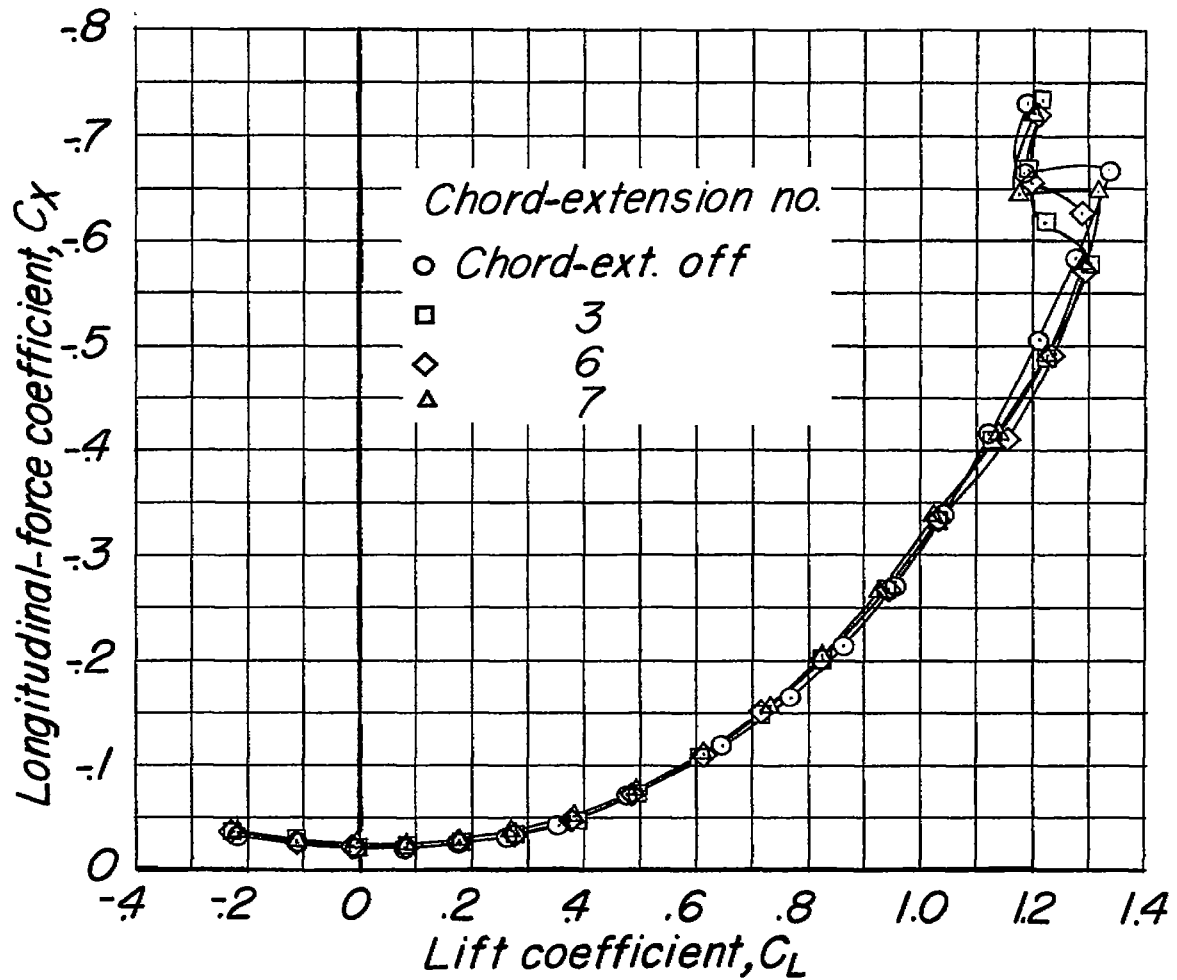
(a) Concluded.

Figure 10.- Continued.



(b) Chord-extensions off and chord-extensions 3, 6, and 7.

Figure 10.- Continued.



(b) Concluded.

Figure 10.- Concluded.

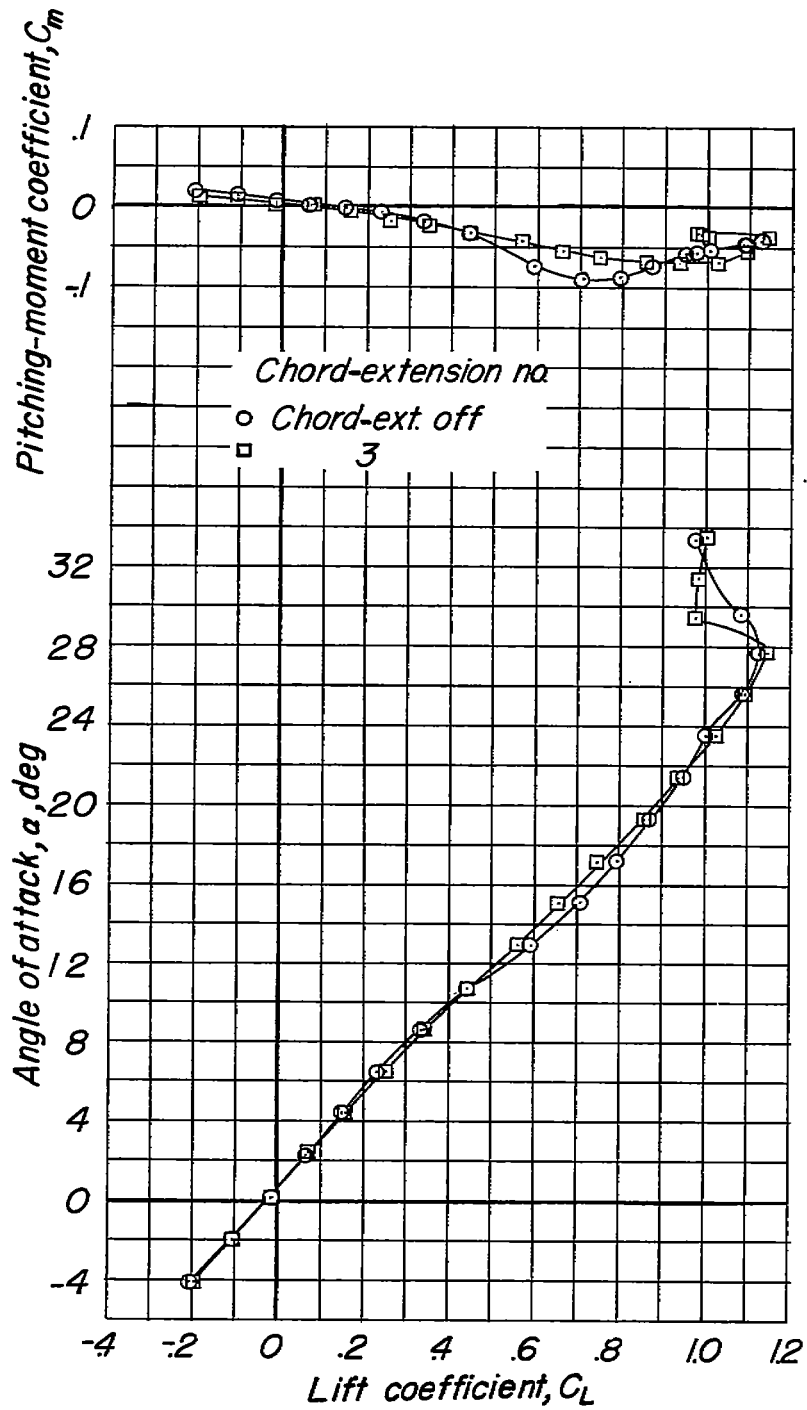


Figure 11.- Effect of chord-extension 3 (inboard end flat and streamwise at 50° sweep) on longitudinal aerodynamic characteristics of test model. $\Lambda = 60^\circ$; horizontal tail off; $\delta_F = 0^\circ$.

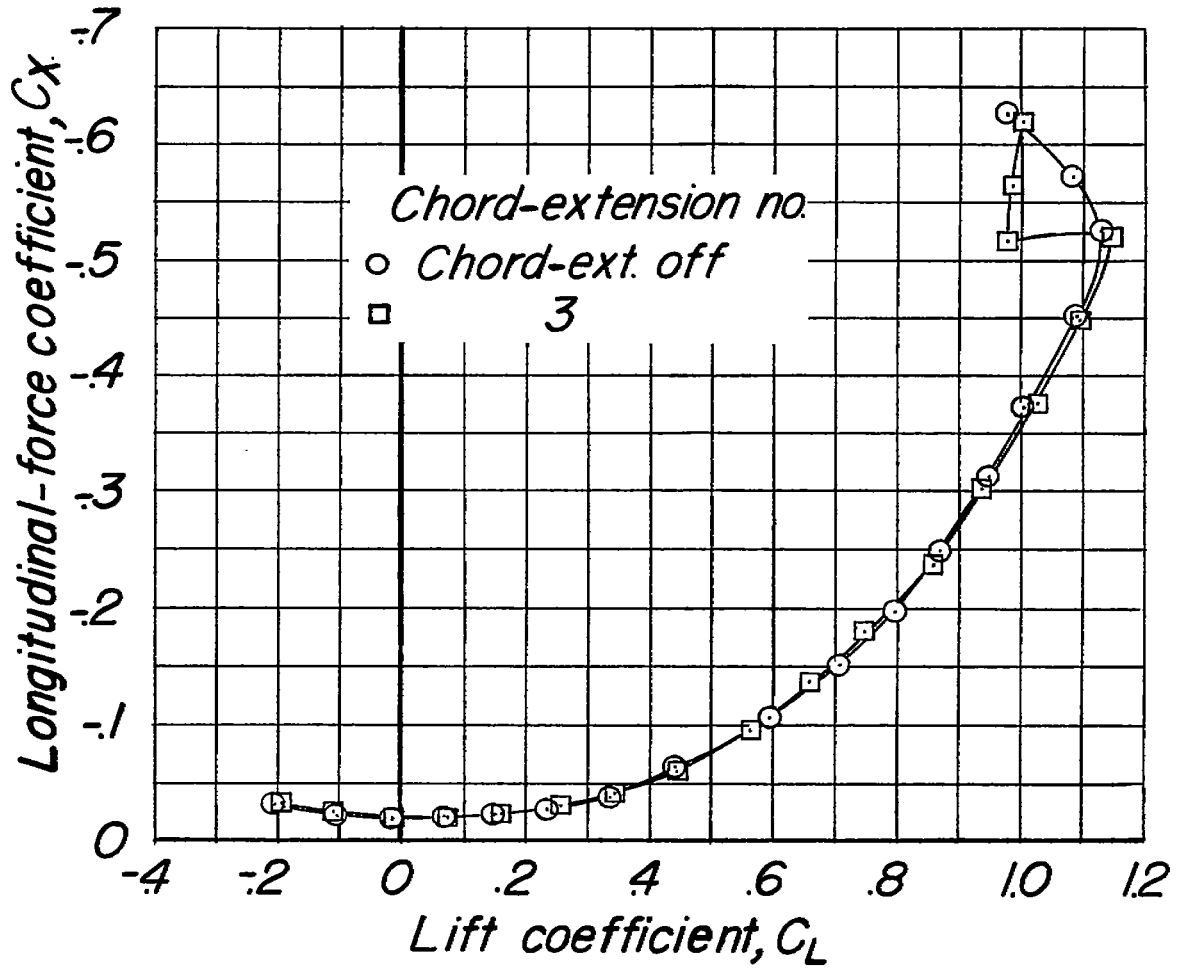


Figure 11.- Concluded.

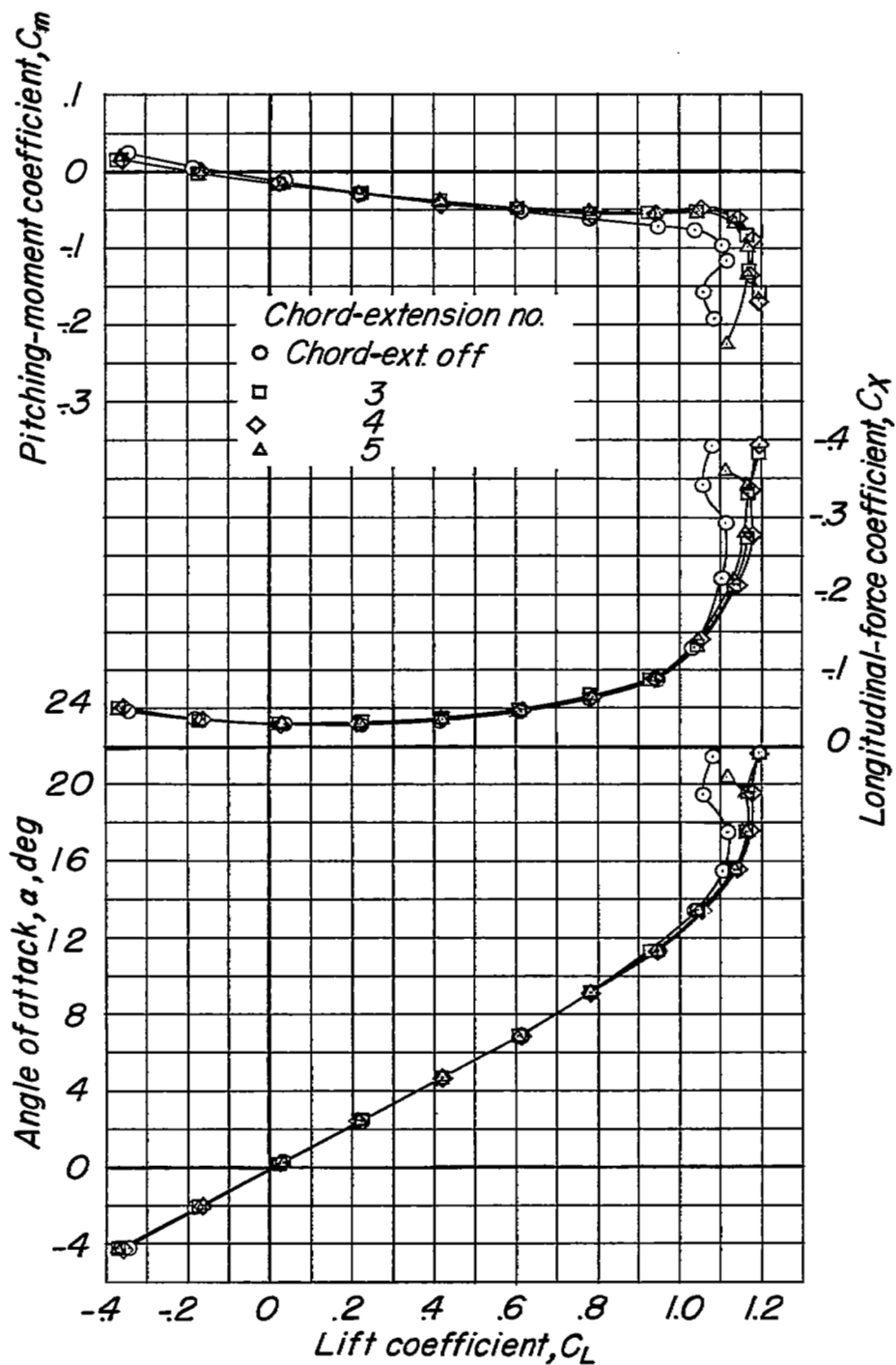


Figure 12.- Effect of several chord-extension configurations on longitudinal aerodynamic characteristics of test model. $\Lambda = 20^\circ$; $i_t = -3/4^\circ$; $\delta_f = 0^\circ$.

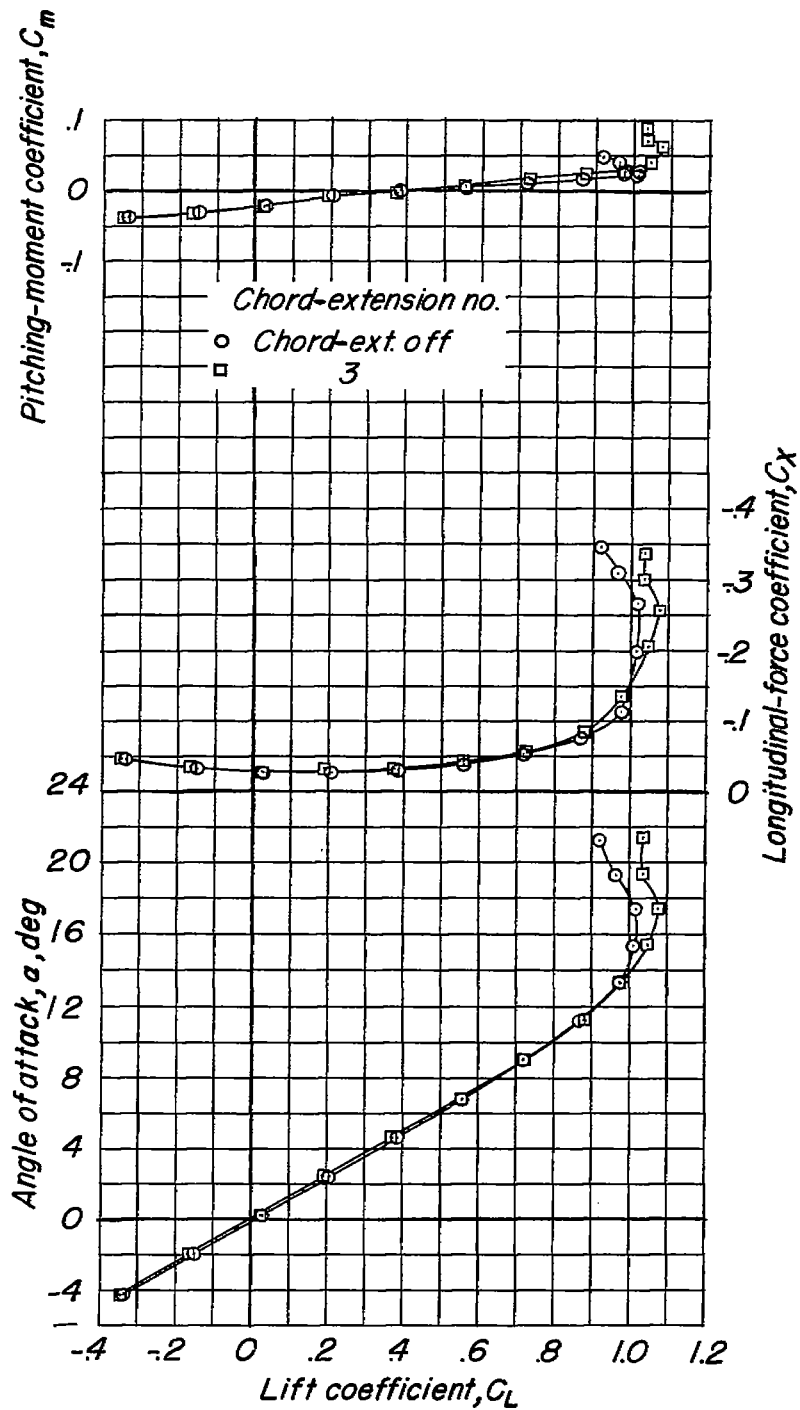


Figure 13.- Effect of chord-extension 3 (inboard end flat and streamwise at 50° sweep) on longitudinal aerodynamic characteristics of test model. $\Lambda = 20^\circ$; horizontal tail off; $\delta_F = 0^\circ$.

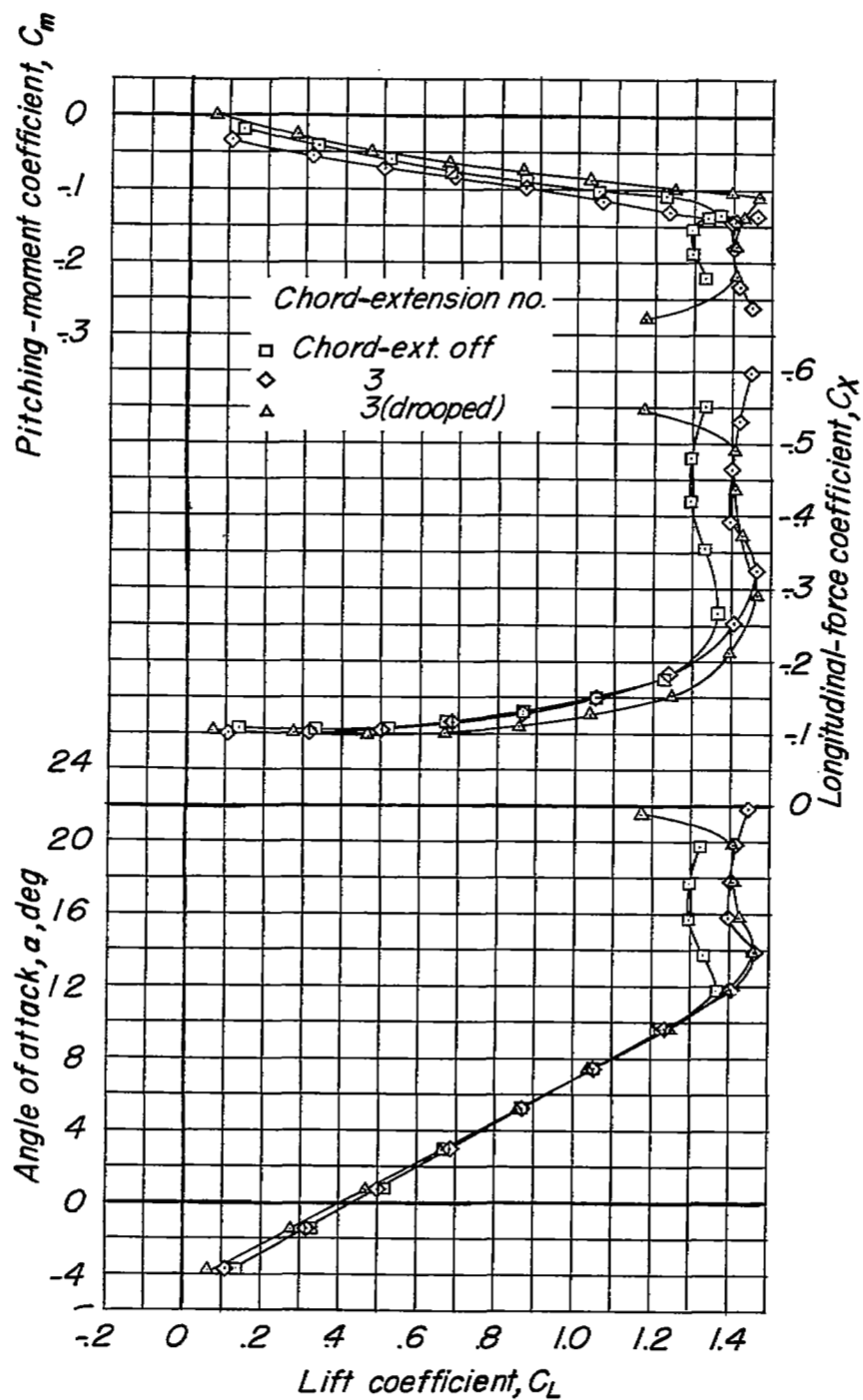


Figure 14.- Effect of chord-extension 3 (inboard end flat and streamwise at 50° sweep) on longitudinal aerodynamic characteristics of test model. $\Lambda = 20^\circ$; $i_t = -3/4^\circ$; $\delta_f = 50^\circ$.

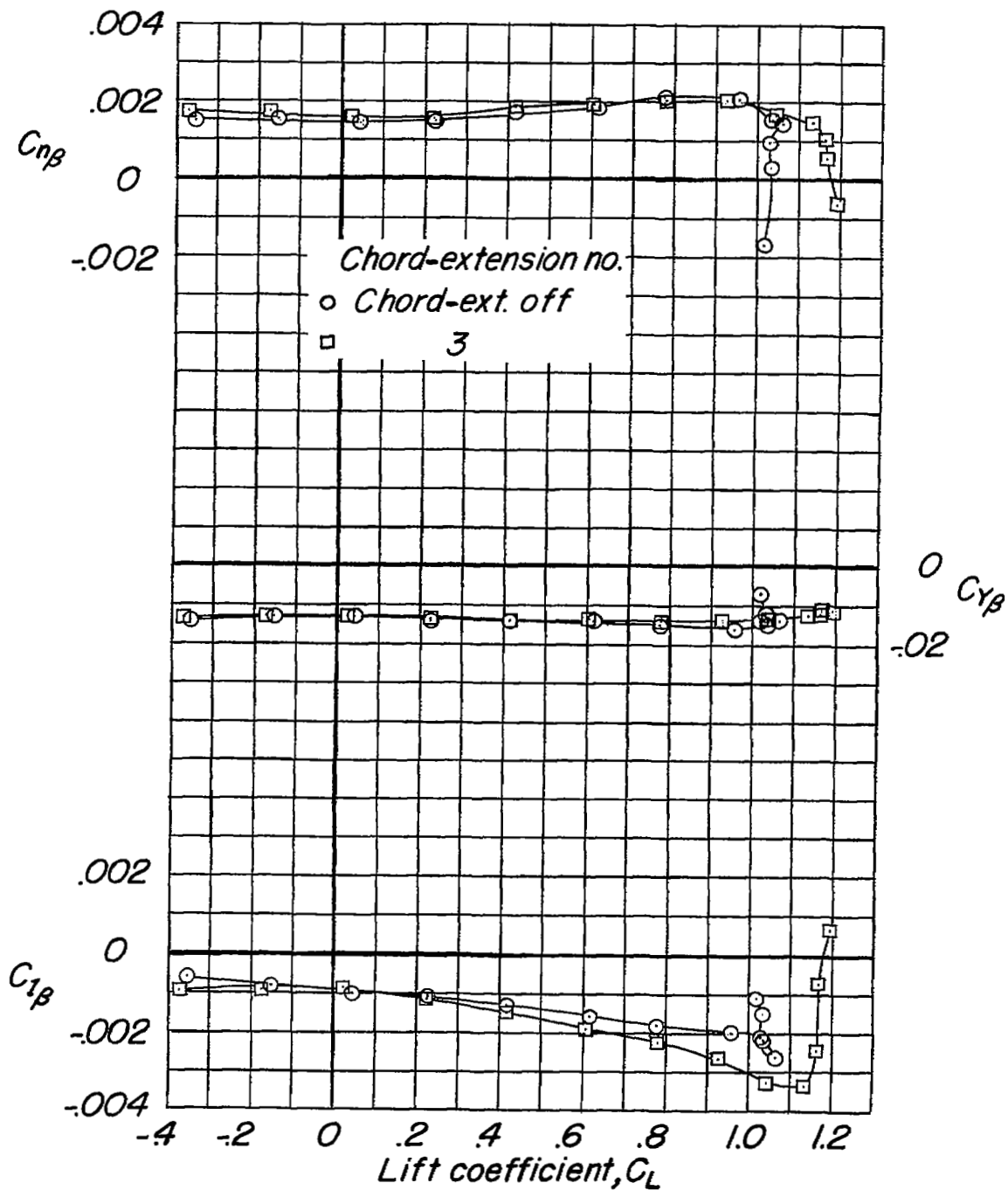
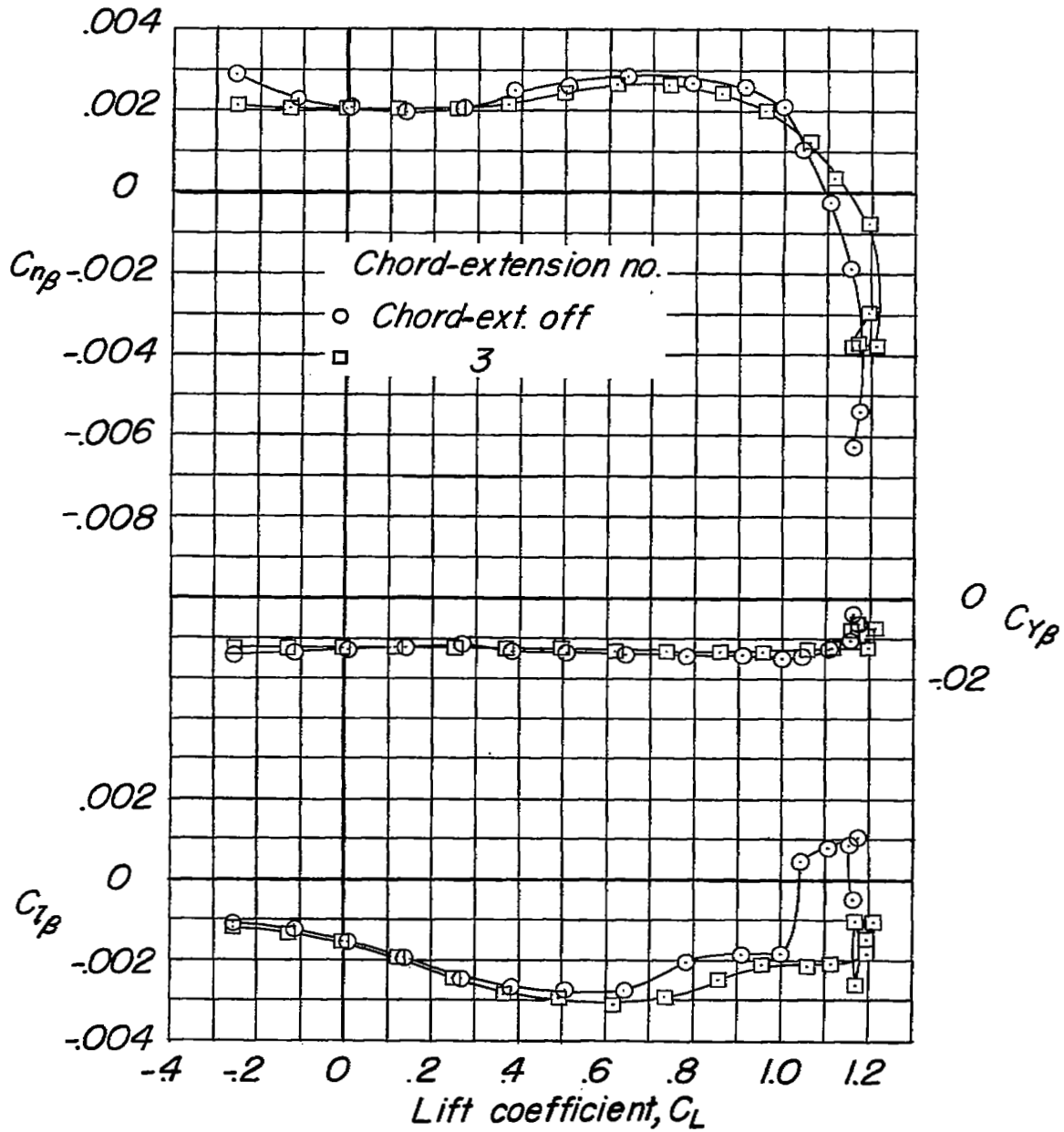
(a) $\Lambda = 20^\circ$.

Figure 15.- Effect of chord-extension 3 (inboard end flat and streamwise at 50° sweep) on lateral stability parameters of test model. $i_t = -3/4^\circ$; $\delta_f = 0^\circ$.



(b) $\Lambda = 50^\circ$.

Figure 15.- Continued.

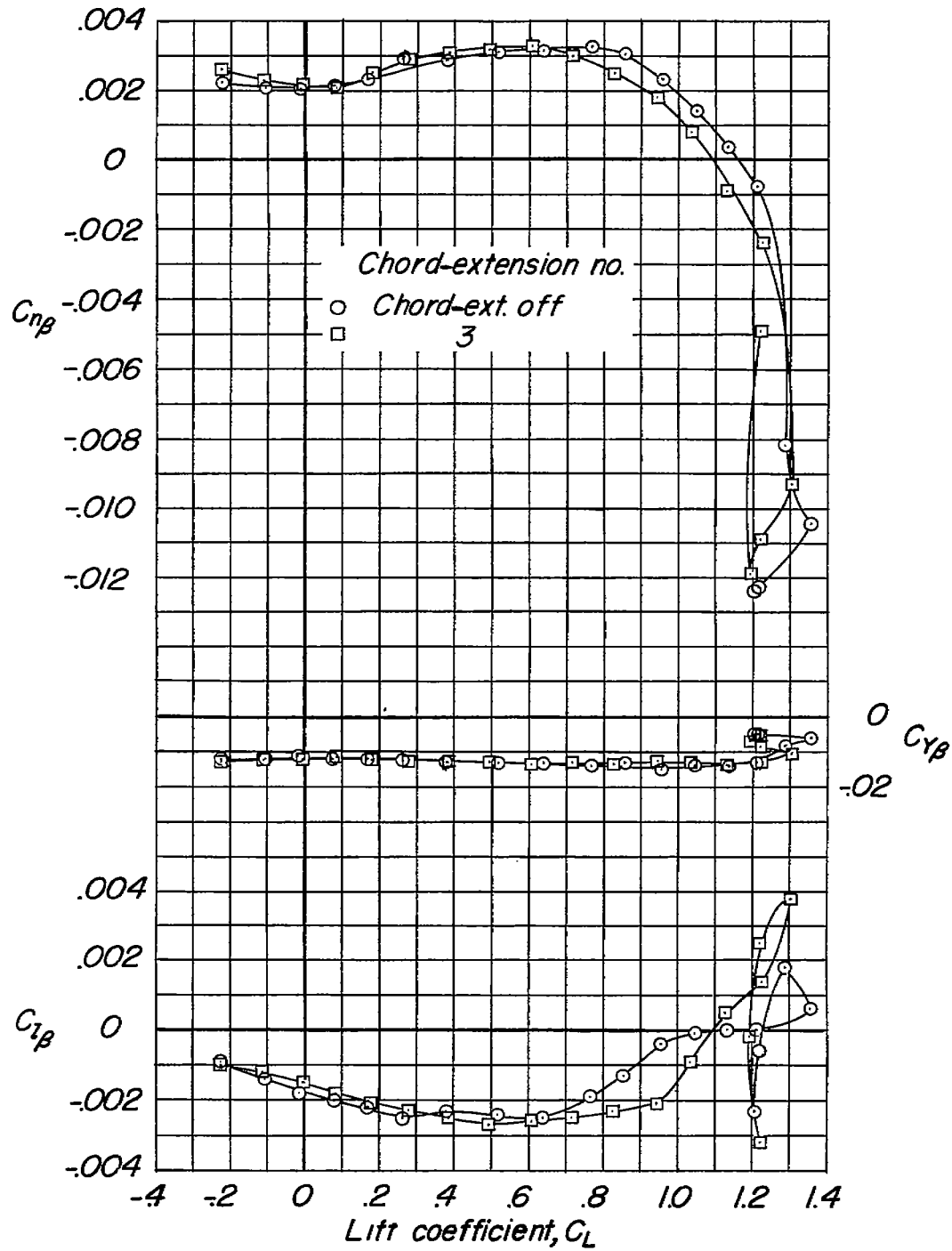
(c) $\Lambda = 60^\circ$.

Figure 15.- Concluded.

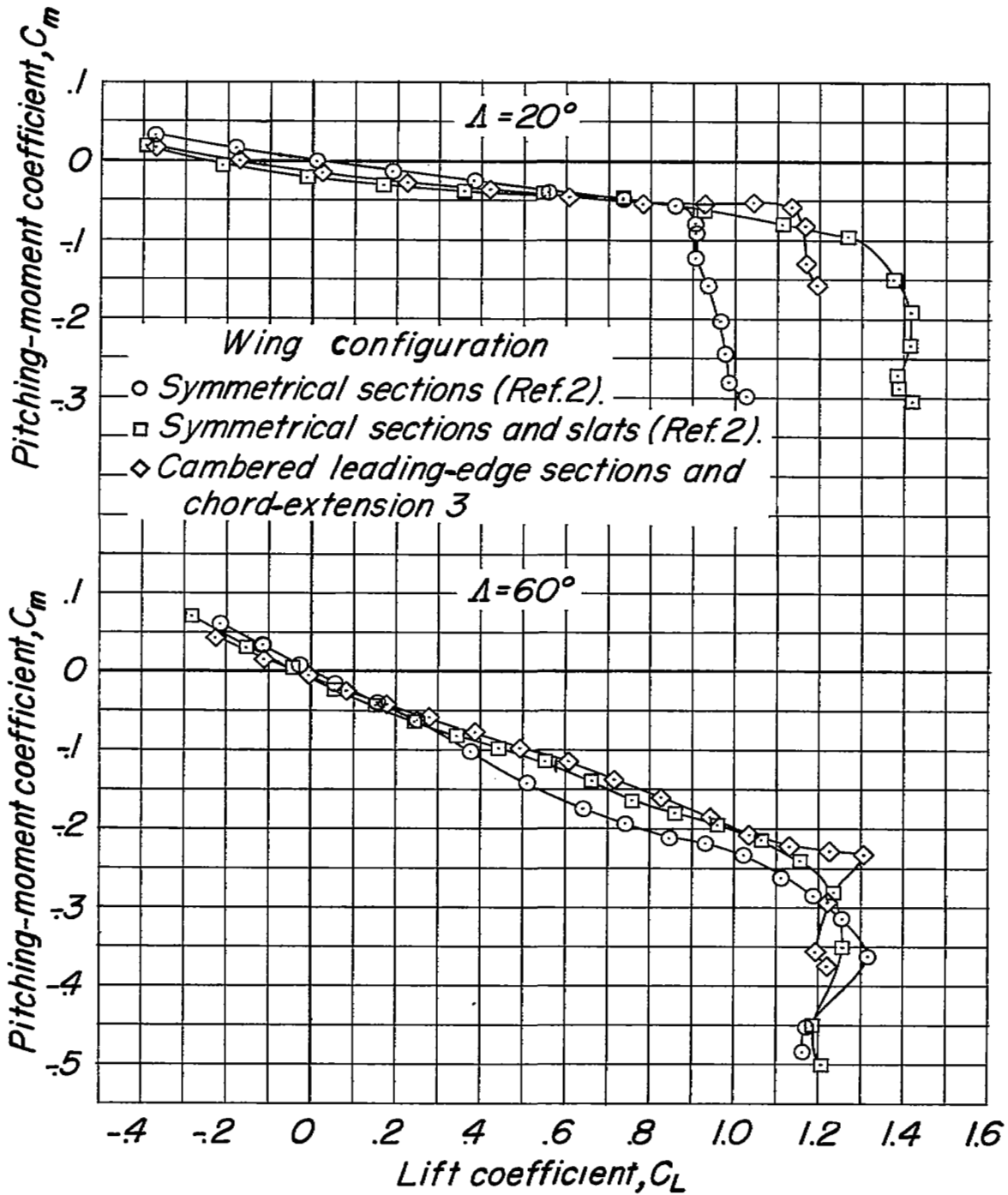
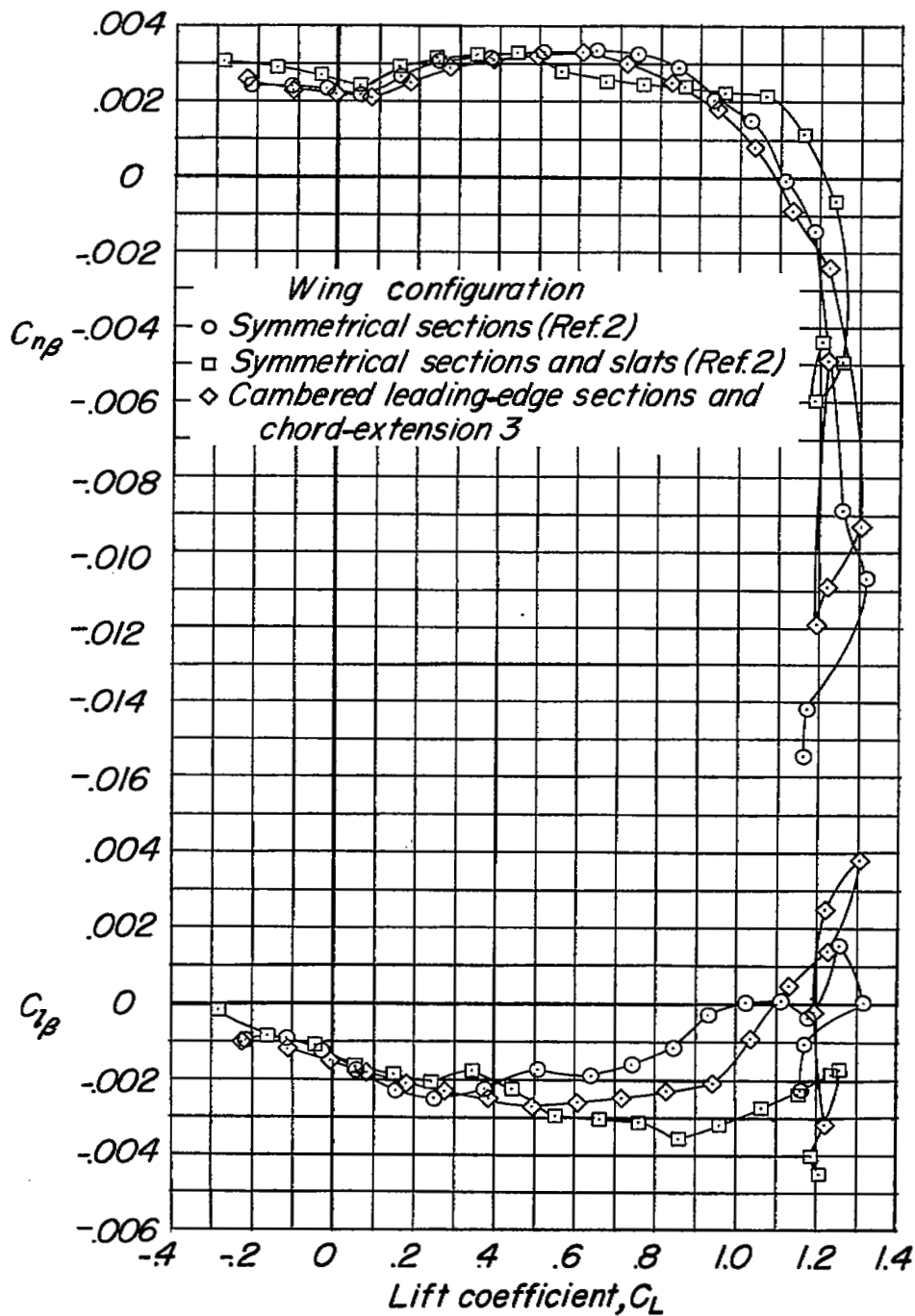
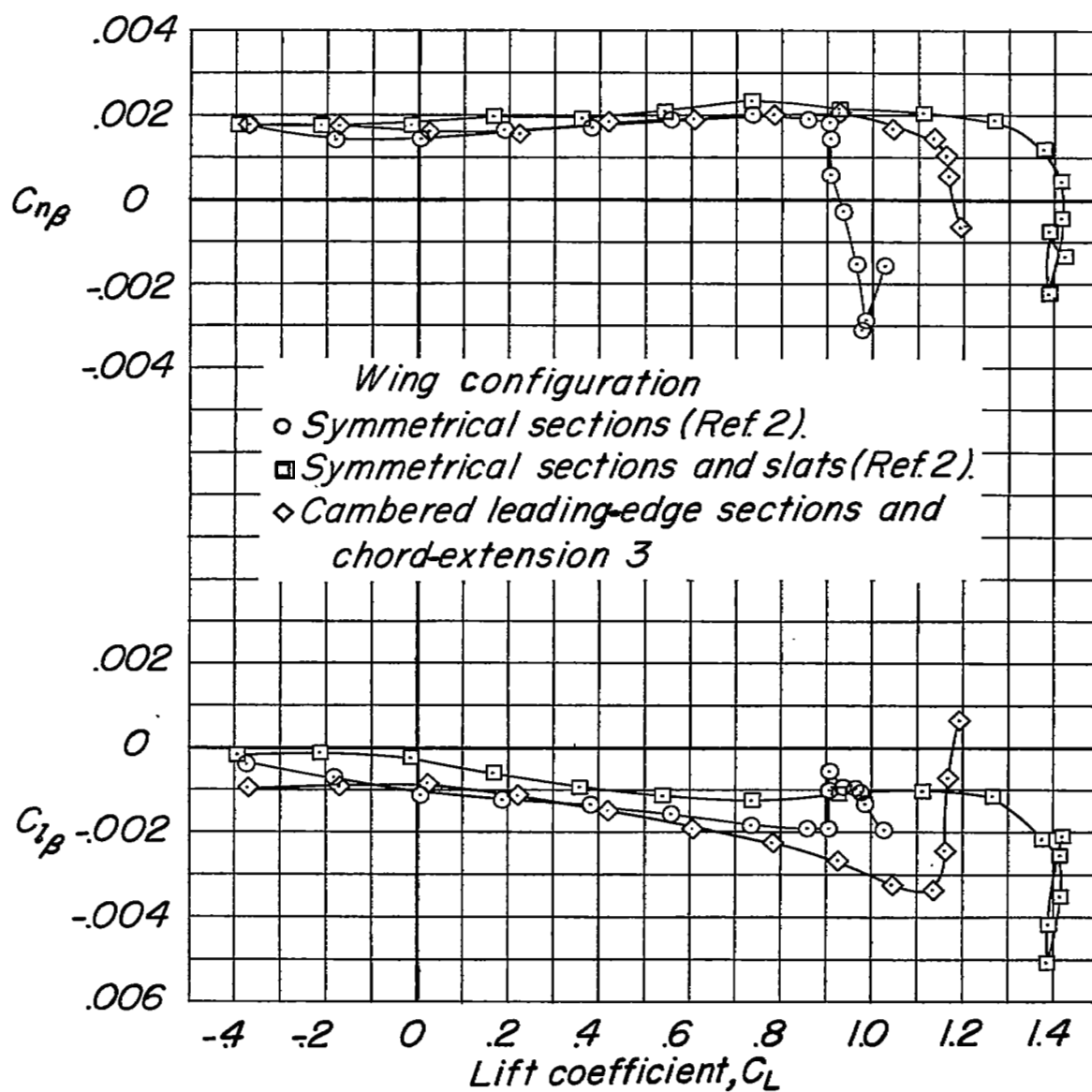


Figure 16.- Effect of several wing configurations on longitudinal stability of test model. $i_t = -3/4^\circ$; $\delta_f = 0^\circ$.



(a) $\Lambda = 60^\circ$.

Figure 17.- Effect of several wing configurations on lateral stability of test model. $i_t = -3/4^\circ$; $\delta_f = 0^\circ$.



(b) $\Lambda = 20^\circ$.

Figure 17.- Concluded.

NASA Technical Library



3 1176 01437 6090

